Geophys. J. Int. (2003) **152,** 139–159

Crustal structure of northwestern Svalbard and the adjacent Yermak Plateau: evidence for Oligocene detachment tectonics and non-volcanic breakup

Oliver Ritzmann and Wilfried Jokat

Alfred Wegener Institute for Polar and Marine Research, Columbusstrasse 27568 *Bremerhaven, Germany.*
E-mails: oritzmann@awi-bremerhaven.de; wjokat@awi-bremerhaven.de

Accepted 2002 July 23. Received 2002 July 18; in original form 2002 March 18

SUMMARY

In 1999 new seismic refraction data were collected off northwestern Svalbard and the adjacent Yermak Plateau. A 260 km long profile provides detailed velocity information for the northeastern edge of the Eurasian Continent and the adjacent Yermak Plateau.

North of Forlandsundet Graben the depth of the Moho varies between 23 and 28 km, and remains at this depth to the northern edge of the profile at 81°N. The crustal lithology off western Svalbard can be related to the basement province west of the Raudfjorden Fault Zone. Off the northern shoreline of Svalbard the structure of the Tertiary Danskøya Basin is mapped. Below this, a Late Silurian/Early Devonian basin, with seismic velocities between 5.1 and 5.8 km s^{-1} and a thickness of up to 8 km is present. A Palaeozoic sequence of up to 6 km thickness is expected below the Tertiary cover north of the Danskøya Basin. An earlier suggestion, that Oligocene rift processes affected the southern Yermak Plateau, is confirmed. A detachment structure is situated below the Palaeozoic Basin below Danskøya Basin, which is probably a consequence of simple shear tectonics. The middle crust exhibits low seismic velocities above the detachment fault. The lowermost crust beneath is slightly contaminated by mantle-derived melts, which is deduced by the slightly elevated velocities of the lowermost crust. These melts can be attributed to decompressive melting caused by modest uplift of the Moho during stretching. The velocity–depth model provides no evidence for large magmatic activity, which implies a non-volcanic rifted margin history. This leads to the assumption that the proposed Yermak Hotspot during the breakup of Svalbard from northern Greenland did not exist.

Key words: crustal structure, extension, hotspots, seismic refraction, Svalbard, Yermak Plateau.

1 INTRODUCTION

The Cenozoic opening of the North Atlantic resulted in the inception of a complex pattern of mid-ocean ridges and fracture zones in the Fram Strait along the northeastern rim of the Eurasian continent (Boebel 2000). The seafloor spreading in the Fram Strait probably occurred less than 20 Ma, and was preceded by oblique stretching and strike-slip movements between Svalbard and northern Greenland (Eldholm *et al.* 1987; Boebel 2000). It has been suggested that the Yermak Plateau and the Morris Jesup Rise (Fig. 1) are both related to hot spot activity during this separation, being two parts of an oceanic plateau found at the Gakkel Ridge plate boundary (Feden *et al.* 1979; Jackson *et al.* 1984).

According to models and observations, where hotspots (mantle plumes) interact with continental margins, their effects are manifested over large distances from the plume head (e.g. 2000 km for the North Atlantic; White & McKenzie 1989; Barton & White 1997). At the outer edges of the plume head magmatism can terminate abruptly, leading to local segmentation of the margin (Barton & White 1997; Skogseid *et al.* 2000). Although a large amount of seismic reflection data exist along the western and northern margins of Svalbard, deep seismic data are sparse. Assumptions concerning the crustal structure and tectonic interpretations of the region are based on limited deep seismic information and airborne potential field measurements (e.g. Jackson *et al.* 1984; Sundvor & Austegard 1990). The objective of this project is to provide new deep crustal information for Svalbard and the Yermak Plateau in order to further constrain their evolution.

Thus, during summer 1999 a deep seismic sounding experiment was performed along the coast of northern Svalbard (Fig. 2) with the German research ice-breaker RV Polarstern. The experimental setup, a dense pattern of onshore and offshore seismic stations in

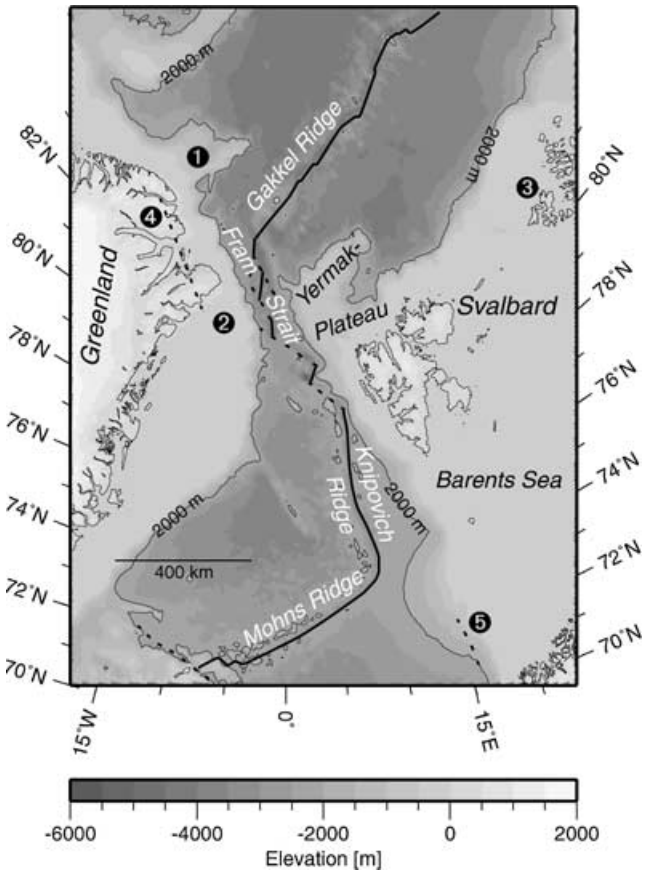

Figure 1. Overview map of the study area. Thick black lines are mid-oceanic ridges, dotted lines indicate transform faults and fracture zones. (1) Morris Jesup Rise; (2) Ob-Bank; (3) Franz-Josef Land; (4) Trolle–Land Fault Zone; (5) Senja Fracture Zone. Bathymetry: IBCAO (Jakobsson *et al.* 2000). Fram Strait plate boundary after Boebel (2000).

combination with a close spacing of airgun shots, was chosen to determine the local velocity distribution of the crust of northern Svalbard and the Yermak Plateau, to better constrain the Palaeozoic to Cenozoic history of the Svalbard region.

Geological setting of western Svalbard and the Yermak Plateau

The archipelago of Svalbard is situated at the northeastern corner of the Barents Shelf of the Eurasian continent (Fig. 1). Northwest of the shoreline of Svalbard the shelves are 50–80 km wide, forming Sjubrebanken, Norskebanken and the Nordaustlandet margin (Fig. 2). Further seawards the hook-shaped submarine Yermak Plateau extends 200 km NNW to 5°E/81.5°N, and then proceeds further 200 km in ENE to 20°E/83°E (Eiken 1993). The northeastern arm of the Yermak Plateau is separated from the Eurasian continental shelf to the south by a 2000–3000 m deep abyssal plain (Fig. 2). To the west of the plateau the 3000 m deep Fram Strait gateway facilitates deep water exchange between the North Atlantic and the Eurasian Basin of the Arctic Ocean (Kristoffersen 1990a; Boebel 2000).

The onshore geology of northwestern Svalbard exhibits a pre-Devonian metamorphic basement province, mainly west of the Breibogen Fault (Fig. 2). In the south this province consists of metasedimentary rocks, and in the centre and north of gneissic, migmatic and related igneous rocks. Overlying this basement is a Late Silurian/Early Devonian sequence, best seen to the east and south of the Woodfjorden area (Hjelle 1979; Harland 1997b). Many authors use the generic term Hecla Hoek for the basement rocks occurring in northern Svalbard. This is a misconception regarding the terrane hypothesis, in which Svalbard is a composite of three allochthonous terranes originating in Greenland, and merged during Caledonian sinistral strike-slip movements. The present relative positions of the terranes were achieved in the Late Devonian. The eastern terrane, related to east Greenland, and the central terrane, related to north Greenland, constitute northwestern Svalbard, i.e. our investigated area. Both terranes are bounded by the postulated Kongsfjorden–Hansbreen Fault Zone (Fig. 2; Harland & Wright 1979; Harland 1997c).

A dredge haul from the central Yermak Plateau yielded high-grade Precambrian gneisses similar to the basement rocks of northern Svalbard (Jackson *et al.* 1984). Further rock samples were collected in 1999 on the northeastern Norskebanken at 16°E and provide low-grade metamorphic rocks (slate dolomite bands), which are suggested to be autochthonous material (Hellebrand 2000).

Offshore geophysical experiments and results

Sparse seismic reflection profiles resolve the sedimentary structure and upper basement character of the continental shelves and the Yermak Plateau. The western tectonic boundary of western Svalbard and the Yermak Plateau is marked by the Hornsund Lineament (Fig. 2; Eiken & Austegard 1987). Structurally, it is a series of blocks, downfaulted to the west between 75°N–79°N along the continental margin. It forms a complex region of crustal transition (Myhre & Eldholm 1988). On northern Sjubrebanken the lineament continues as two separate NNW-trending blocks, approximately 30 km wide, as far as at least 80.5°N (Eiken 1993; Geißler 2001). Eastward, along strike from the lineament on Sjubrebanken a 10 km wide graben filled with Tertiary sediments is probably the northward equivalent of the Tertiary Forlandsundet Graben (Eiken 1993).

The southern Yermak Plateau is generally covered by sedimentary deposits more than 1000 m thick. Only one local outcrop of basement or pre-Cenozoic sedimentary rocks is known, the north-trending H.U. Sverdrup Bank (Fig. 2). Its composition is poorly known. Suggestions range from Precambrian rocks to highly consolidated sedimentary strata of various ages and tectonic origins (Eiken 1993). A striking feature of the southern plateau is the 4000–5000 m deep Tertiary Danskøya Basin, which strikes obliquely (30°–35°) to the main fault pattern of the Hornsund Lineament (Fig. 2). Subsidence and sedimentation is believed to have started at the end of the Eocene (36 Ma) and was superimposed by syn- and post-depositional uplift of northwestern Svalbard. Eiken (1993) suggests a transtensional mechanism with resemblance to pull-apart for the Danskøya Basin. Between 12°E–18°E at the landward reaches of Norskebanken the Moffen Fault acts as a hinge between continental crystalline rocks and the shelf sedimentary layers.

Deep seismic investigations were first performed in 1976 to investigate the crustal structure of Svalbard and its adjacent regions (Guterch *et al.* 1978). The area investigated (central Svalbard and Isfjorden) is located 50–80 km beyond the southern edge of our new profile AWI-99300. This provides basic information on crustal thicknesses in an area not affected by Tertiary rift events.

Chan & Mitchell (1982) published a three-layer crustal velocity model with a total thickness of 27 km beneath northern Isfjorden. This 1-D model was correlated with a petrological model derived from deep crustal and mantle xenoliths of the Neogene volcanic

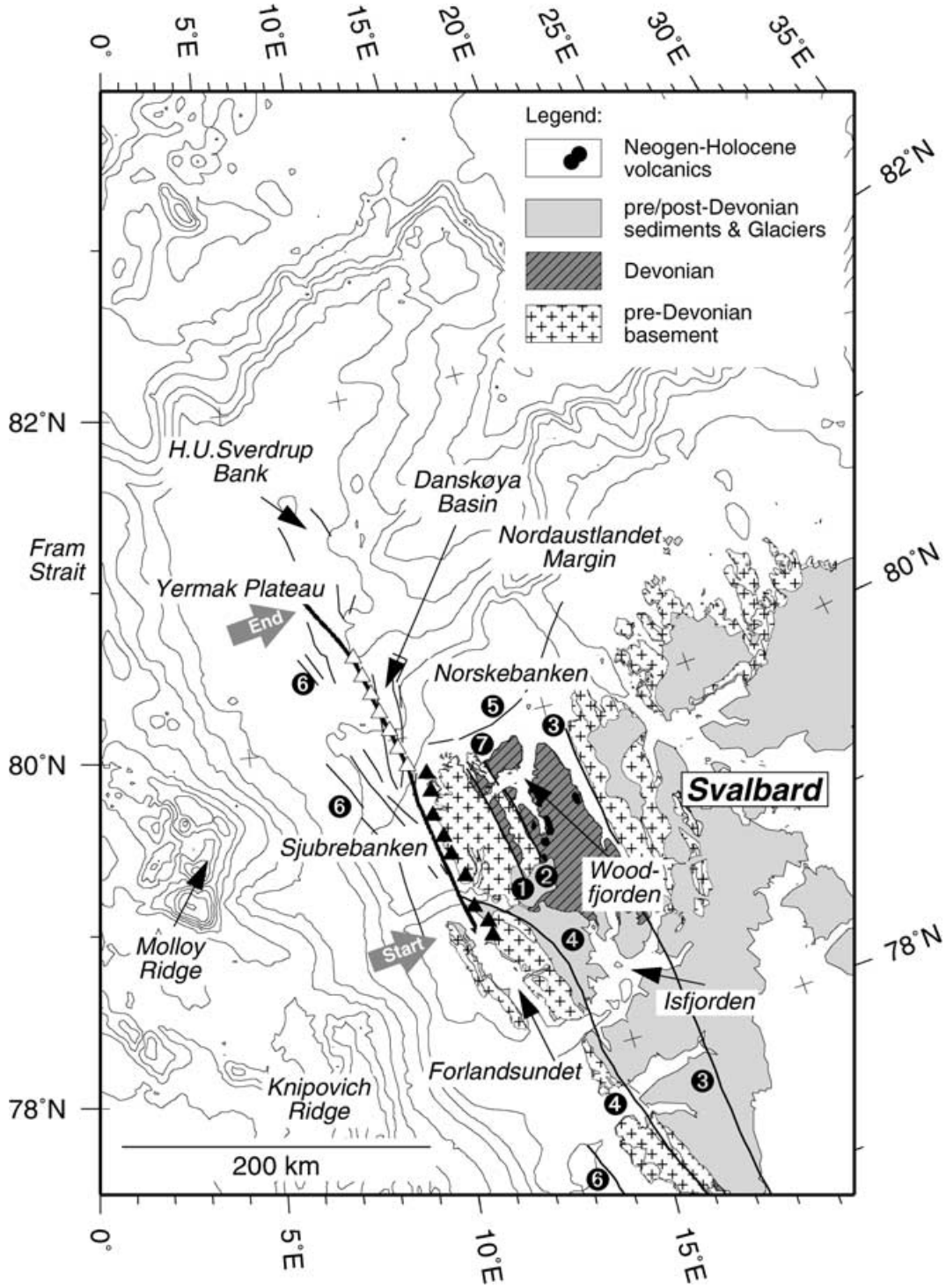

Figure 2. Location of seismic refraction profile AWI-99300. The profile is marked by a thick black line (offshore), RefTek- and OBH stations by black and white triangles, respectively. Geology: Harland (1997a). Black lines are major faults onshore and offshore, numbered circles mark the following structures: (1) Raudfjorden Fault Zone, (2) Breibogen Fault Zone, (3) Billefjorden Fault Zone, (4) Kongsfjorden–Hansbreen Fault Zone, (5) Moffen Fault, (6) Hornsund Lineament, (7) Siktefjellet Strike–Slip Zone. Note, that the (sinistral strike-slip) faults (3) and (4) are proposed to subdivide Svalbard into the western-, central- and eastern terrane. Bathymetry: 500 m-interval + 200 m-contour (IBCAO; Jakobsson *et al.* 2000).

centres in northwestern Svalbard (Amundsen *et al.* 1987). In the model the rock types change from gneissic to granulitic at depths of approximately 14 km, which correlates well with the velocity model. Above the crust–mantle boundary lies a 6 km thick transition zone, suggested to include significant interlayered mantle pyroxenites and/or lherzolites. 2-D velocity models were published by Sellevoll *et al.* (1991), presenting a crustal thickness of 36 km for the Isfjorden area, based on the same data set used by Chan

& Mitchell (1982). A thickness of 26 km was modelled below the Forlandsundet Graben. Owing to an insufficient number of shots and receivers it was not possible to resolve a detailed velocity–depth function along the profiles. Despite this setup, lateral velocity variations in the deeper crust, occurring below the major fault zones of Svalbard, are reported.

Czuba *et al.* (1999) compiled Polish research activities on the crustal structure of Svalbard from 1978 to 1985 and proposed a two-layer model for the Isforden/Forlandsundet area. A significant difference with respect to older models is a 12 km thick lower crustal layer, of high seismic velocities up to 7.2 km s^{-1}. This layer is modelled up to western Norskebanken, where seismic velocities increase to 7.35 km s^{-1}. Gravity modelling (Myhre & Eldholm 1988; Sundvor & Austegard 1990; Austegard & Sundvor 1991) confirms the seismic crustal thicknesses for the western Svalbard and coastal regions, but could neither confirm nor disprove the existence of a high-velocity/density body in the lower crust.

Jackson *et al.* (1984) published two unreversed seismic refraction lines north of 81°N on the Yermak Plateau. Two crustal layers, showing seismic velocities of 4.3 and 6.0 km s^{-1} and a crust–mantle boundary at approximately 20 km were modelled. According to this model, the crust thins sharply north of 82°N. Velocities of the basement of the southern Yermak Plateau, derived from sonobuoy data suggest a continental crystalline crust for this area (Sundvor *et al.* 1982). Boebel (2000) provides additional evidence for the continental nature of the southern and central Yermak Plateau from gravity modelling.

Cenozoic tectonic evolution

The earliest dextral strike-slip movements between Svalbard (Eurasia) and Greenland began 80 Myr (chron 33) in the Late Cretaceous, along the Trolle–Land Fault Zone in northeast Greenland (Fig. 1; Håkansson & Pedersen 1982). Eldholm *et al.* (1987) propose this fault to be the continuation of the Senja Fracture Zone of the North Atlantic. Throughout this strike-slip zone, local pull-apart basins developed. A short-lived change of spreading direction in the Labrador Sea west of Greenland gave rise to a brief period of Palaeocene compression (59–56 Ma; chron 25, 24), affecting the juvenile transpressive fold belt of western Spitsbergen (Müller & Spielhagen 1990). Simultaneously, true seafloor spreading to the south occurred only at Mohns Ridge, while rifting and crustal extension continued in the juvenile Norwegian–Greenland Sea. Later strike-slip movements occurred along the Hornsund Lineament, east of the Trolle–Land Fault Zone (Eldholm *et al.* 1987). Immediately following Early Eocene times (56 Ma, chron 24) the western margin of Svalbard entered a transpressive regime, which sustained orogenic activity in the fold belt (Steel *et al.* 1985). The development of the juvenile Eurasian Basin began with spreading at the Gakkel Ridge (56 Ma, chron 24; Kristoffersen 1990b). Transpression in western Svalbard was replaced by transtension in the middle Eocene (49 Ma, chron 21). For this period Crane *et al.* (1991) suggest pull-apart and (later) spreading processes at the Molloy Ridge as an extensional relay zone in response to the readjustment of the Nansen Ridge and/or the Mohns Ridge.

Transtensional movements dominate since the earliest Oligocene (36 Ma, chron 13). Authors agree that the lithosphere west of the Hornsund Lineament was stretched and later rifted (e.g. Eldholm *et al.* 1987; Müller & Spielhagen 1990; Crane *et al.* 1991; Boebel 2000). In addition, Feden *et al.* (1979) and Jackson *et al.* (1984) propose mantle plume activity (the Yermak Hot Spot) at a former triple junction position at the eastern end of the Gakkel Ridge during this period. This triple junction was formed by the juvenile Gakkel Ridge and Hornsund Lineament and a transform fault cutting Ellesmere Island from northern Greenland. It is suggested that excessive magmatism, associated with the mantle plume built up the northern Yermak Plateau and Morris Jesup Rise. The northeastern plateau shows a pronounced high-amplitude, long-wavelength magnetic anomaly (the Yermak Anomaly; Feden *et al.* 1979). This anomaly, compared with the quiet magnetic signature south of 82°N, leads to the suggestion that the plateau had a dual origin. The northeastern part consists of thickened oceanic crust created by hotspot activity, whereas the southern part is continental (Jackson *et al.* 1984). Transtensional processes 36 Ma led to the beginning of subsidence in the Danskøya Basin on the southern plateau, which resembles a pull-apart structure (Eiken 1993).

The precise geodynamic history of the Fram Strait oceanic province west of the Yermak Plateau is still under debate (e.g. Srivastava & Tapscott 1986; Lawver *et al.* 1990; Sundvor & Austegard 1990; Boebel 2000).

According to the model of Boebel (2000), a transtensional tectonic regime lasts up to the Middle Miocene (12 Ma, chron 5) at the western rim of the Yermak Plateau (Hornsund Lineament). Seafloor spreading began at the northern Knipovich Ridge in the Late Oligocene (25 Ma) and on Molloy Ridge in the Early Miocene (20 Ma). The generation of new crust along two proposed oblique spreading mid-ocean ridges in the northern Fram Strait, balanced the dextral movements of Svalbard relative to Greenland since the Late Miocene between 12 and 9.5 Ma (chron 5). Feden *et al.* (1979) suggested renewed plume activity along the western segment of the Gakkel Ridge since chron 5, which is supposed to stimulate Tertiary/Quaternary volcanic activity, i.e. basaltic flows/upper-mantle xenoliths in northern Svalbard.

2 NEW GEOPHYSICAL DATA

Acquisition of seismic refraction data

Seismic refraction data along profile AWI-99300 were acquired by the German polar icebreaker RV Polarstern in 1999 August. The seismic source, fired every minute (∼150 m interval), consisted of two large volume airguns with a total volume of 92 l. The 260 km (=1475 shots) long seismic transect follows the coastline of western Spitsbergen north of Prins Karls Forland towards the Yermak Plateau (Fig. 2). Nine RefTek seismometer stations with a receiver spacing of 9–20 km were deployed on the coast of Spitsbergen to record the seismic energy. This setup resulted in minimum shot–receiver offsets of 6–10 km for RefTek land stations, as the source (RV Polarstern) was situated offshore. The chosen station locations did not exceed altitudes of 70 m asl. Each station was equipped with 18 single-coil geophones (4.5 Hz) and the signals were stacked. On the southern Yermak Plateau seven ocean-bottom hydrophone systems were deployed with a mean spacing of 13 km in water depths of 400–950 m bsl (Fig. 2).

Beside the use of airguns as an energy source the Polish ship El Tanin performed 20 TNT-shots with a charge of 25/50 kg north of 79.8°N and a shot distance of approximately 7 km. The seismic energy of the airgun source was strong enough to provide a high signal-to-noise ratio on the recordings, so that the TNT-shots give no supplementary information for crustal studies. Therefore, the seismic sections presented in this publication contain recordings of the airgun source only.

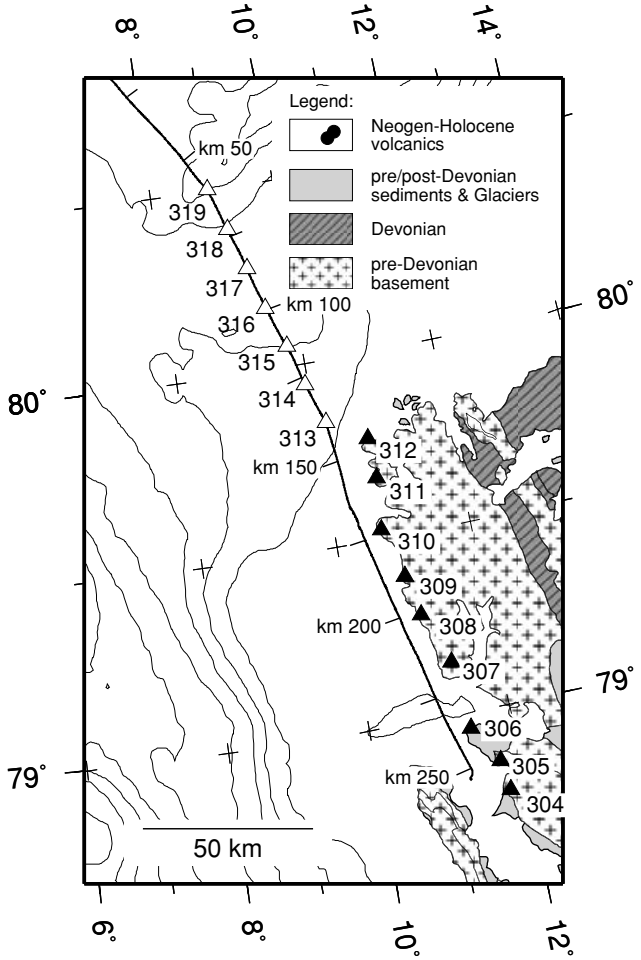

Figure 3. Locations and names of deployed seismic stations during the AWI-99300 experiment. Black triangles mark the position of onshore RefTek seismometer stations. White triangles mark the positions of offshore ocean-bottom hydrophone systems. Geology: Harland (1997a). Bathymetry: 250 m-interval (IBCAO; Jakobsson *et al.* 2000).

Examples of seismic refraction data

In this section we present six (of a total of 16) seismic sections recorded during the AWI-99300 experiment. The sections shown are representative examples, which explain the main features of acquired data (Figs 4a–f: ref304, ref306, ref311, obh313, obh317 and obh319, below).

The seismic refraction data recorded by the RefTek stations onshore (ref304–312; for locations see Fig. 3) are generally of good quality over almost the entire profile length on either side of the receivers (up to 140–240 km offset; Figs 4a–c). The ocean-bottom receiver systems on the Yermak Plateau (obh313–319; for locations see Fig. 3) provide variable quality between 40–140 km offset and a signal-to-noise ratio of approximately 1 at some stations (Figs 4d–f). Thus, arrivals were only detected by phase correlation, facilitated by the close shot spacing.

The frequency spectra of the recorded data are in the range of 5–15 Hz with a dominant peak at 8 Hz. A bandpass filter passing frequencies from 5 to 17 Hz (the exception is obh315: 11–20 Hz) was applied to the data. For further enhancement of reflected and refracted arrivals at offsets greater than 20 km, the data were scaled by automatic gain control within a window of 1000 ms.

The recorded wavefield is characterized by a strong reverberation pattern, probably created by the multiple reflection of the source signal off the ocean floor in shallow water. A large impedance contrast is given by known high-velocity gas hydrate cemented sediments on the oceanfloor off northwestern Svalbard (Posewang & Mienert 1999). In addition, high seafloor velocities are supposed to result from overconsolidation associated with Late Cenozoic uplift of the shelf areas (e.g. Eiken & Austegard 1987). Peg-leg-type propagation of seismic energy can further be induced by the occurrence of low-velocity gas bearing sediments below these horizons at depths of 100–200 m bsf. Despite this, first arrivals and sedimentary and crustal reflections are clearly observed on many of the sections (e.g. obh313; Fig. 4).

Owing to the chosen shot interval of 60 s, noise from the previous shot overprints useful signals at distances of approximately 90 km in the case of some of the ocean-bottom receivers, e.g. obh313 (15–60 km; Fig. 4d). The recordings of the RefTek stations are not affected by this kind of noise energy.

At the southern end of the profile at Kongsfjorden the recordings ref304–306 show refracted phases at near offsets (<15 km) with a high gradient and seismic velocities of 4.5–5.0 km s^{-1} (Figs 4a and b). At larger distances to the receiver the gradient decreases and crustal *p*-phases are only affected by moderate lateral heterogeneity of the crust on the southern Yermak Plateau. These undulations of the apparent velocity, i.e. positive or negative slope changes occur between 110–180 km along the profile (e.g ref306; Fig. 4b). Crustal *p*-phases (diving waves) often remain beyond the crossover distance of mantle phases as secondary arrivals and give reliable information concerning seismic velocities and gradients in the deeper crust, e.g. ref311 (Fig. 4c).

On the southern Yermak Plateau the near offsets (<15 km) of the recordings ref312–obh316 (for example, Figs 4c and d; p1) show arrivals from the sedimentary cover on the shelf and the Danskøya Basin identified by low seismic velocities of 2–3 km s^{-1} and a high-velocity gradient. Owing to the thinning of the Tertiary sediments north of Danskøya Basin crustal *p* arrivals occur increasingly earlier on more northern stations.

On all stations deployed on Spitsbergen and on some ocean-bottom stations (e.g. obh314/317) refracted seismic signals from the upper mantle (p_n > 7.8 km s^{-1}; Figs 4a–c), and mantle wide-angle reflections, were recorded. The crossover distance remains rather constant at 90–110 km on all stations, which points to a uniform Moho depth. Amplitudes of p_n arrivals are, in relation to crustal *p* arrivals obviously lower. This is probably caused by a very low-velocity gradient in the upper mantle.

Converted *s*-wave energy is recorded on only some of the receivers (Figs 4a and b; s2). *S*-wave arrivals, which occur in a diffused pattern of high-energy *p*-wave reverberations of reflections, are not easy to define on these stations (Fig. 4a). Owing to only a few *s*-wave arrivals and the described difficulties we cannot derive an *s*-wave velocity model and Poisson's ratio, which would have given further constraints for a rheologic interpretation.

Gravity data

Gravity data were acquired in parallel with seismic measurements by the shipboard gravity meter KSS31 (Bodenseewerke). The data were linked to the International Gravity Standardization Net 1971 (IGSN71) using harbour measurements in Tromsø (Norway). The observed gravity was resampled to a 2 km interval, which is reasonable for resolving large-scale sedimentary structures and crustal

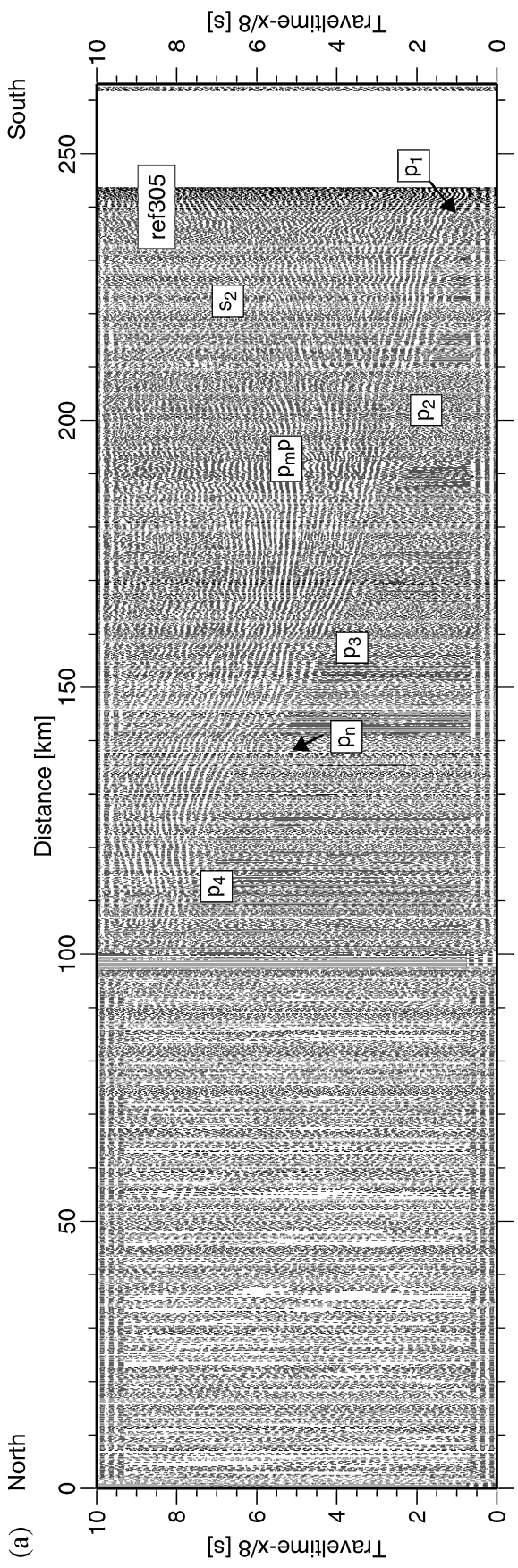

Figure 4. Representative record section examples for onshore and offshore receivers (a–c: RefTek seismometer systems ref305, ref306 and ref311; d–f: ocean-bottom hydrophone systems obh313; obh317 and obh319). For processing details see the text.

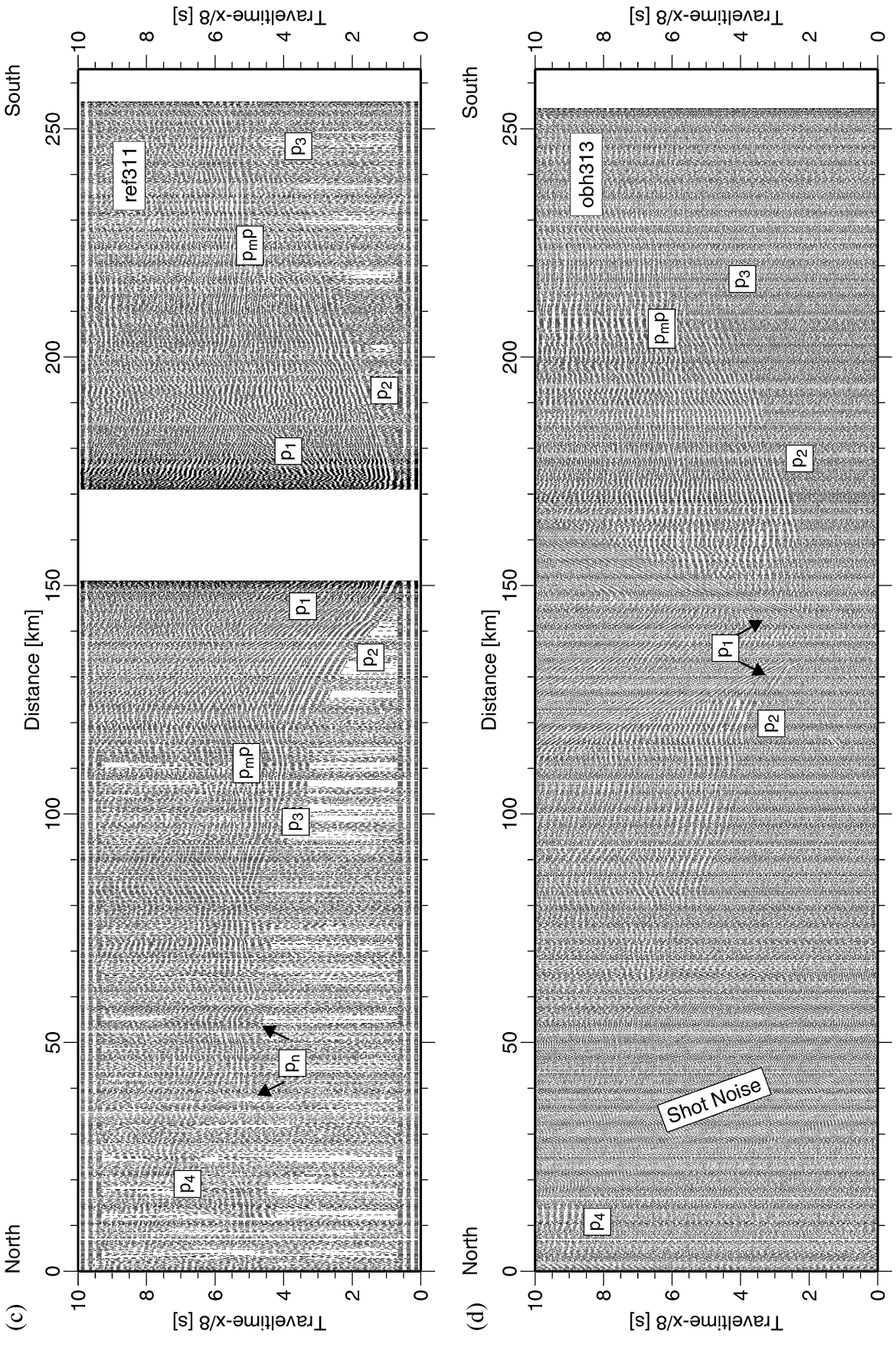

Figure 4. (*Continued.*)

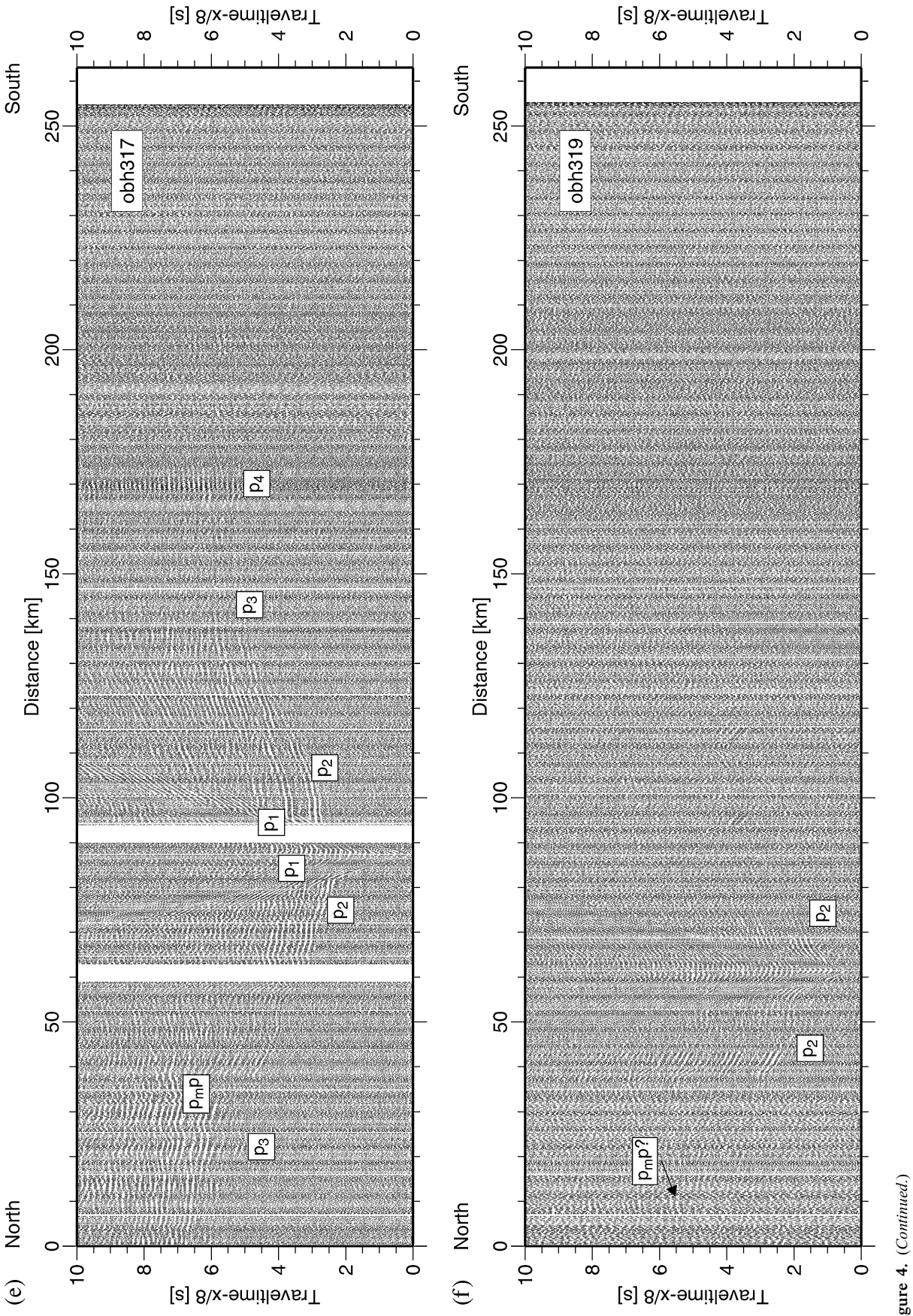

Figure 4. (*Continued.*)

structures. The applied processing sequence comprises latitude and Eotvoes correction to calculate the free-air anomaly.

Since the ship passed significant coastal topography at distances of approximately 10 km, possible terrain effects had to be checked. A test was conducted on the free-air anomaly grid of the Fram Strait, Svalbard and northeast Greenland (Boebel 2000). A terrain correction was calculated by fast Fourier transformation (Forsberg 1984). The calculated influence on gravity measurements at 10 km distance was less than 0.75 mGal, less than 1.5 per cent of the maximum gravity variation in the gravity value measured by the ship along our profile track. Furthermore, this correction is smaller than the gravity variations caused by the uncertainty of the initial density model, which is itself derived from wide-angle data modelling. The effect of the surrounding terrain on the gravity values measured by the ship are therefore insignificant for crustal investigations.

3 VELOCITY MODELLING

Modelling procedure

For modelling the RefTek/OBH wide-angle data we used the following strategy. (1) Traveltimes of refracted and reflected arrivals with good correlation were picked on each of the 16 recordings. (2) 1-D velocity profiles were calculated for each station and gathered to a 2-D velocity section, which was used as the initial model for raytracing. (3) The program rayinvr (Zelt & Smith 1992) was used to perform 2-D raytracing with a forward modelling technique. The modelling procedure took place layer by layer, starting from the top. The parametrization of the velocity model (depths and velocities), was held fixed when the next layer was modelled. To fit the traveltimes taken from the seismic recordings some additional velocity or boundary nodes were implemented in the velocity model. During modelling more emphasis was put on matching the slope and shape of the observed traveltime branches than on minimizing the traveltime residual provided by the program rayinvr. (4) After producing a reliable model, traveltimes were calculated for phases of stations that reveal poorer quality caused by lower signal-to-noise ratios. A second inspection of the data was conducted to search for 'hidden' information, such as low-amplitude arrivals. (5) The final fit of observed traveltimes was derived by two runs of the inversion method of rayinvr to the velocity model.

The observed and calculated traveltimes of the final *p*-wave velocity model are shown in Fig. 5. In total, approximately 4200 traveltimes of refracted and reflected energy were picked from the seismic section and used for raytracing. The corresponding raypaths are shown in Fig. 6.

Several seismic record sections show diffraction arrivals at traveltimes before and after P_mP arrivals, which are concentrated on the southern Yermak Plateau. Attempts to model the locations of diffraction origins derived no consistent results. This may point to a complex 3-D structure in the central section of the profile.

Final velocity model

The final velocity model for the profile AWI-99300, shown in Figs 7 and 8, is composed of five layers excluding the water column. The uppermost of four crustal layers was inserted for the sedimentary section (Fig. 7), while below, three layers represent the crystalline section and highly consolidated sedimentary rocks of the crust (Fig. 8). The lowest layer represents the upper mantle. Within each layer, the seismic velocities vary both horizontally and vertically.

Tertiary Sedimentary Section. Seismic velocities for the 2 km thick sedimentary sequence on the shelf (145–160 km) vary between 2.6 and 3.0 km s^{-1} at the seafloor and 4.1 and 4.8 km s^{-1} at the lower boundary. Tertiary sediments thicken towards the north in the southern Danskøya Basin to a maximum of 3.0–4.5 km (Fig. 7). The base of the sediments in the Danskøya Basin is formed by a 70 km wide w-shaped boundary. Seismic velocities of 2.0–3.0 km s^{-1} at the top and 3.3–4.3 km s^{-1} at the base of the sequence are calculated. The thickness of the Tertiary sedimentary section north of Danskøya Basin (60 km) is not well constrained, owing to the lack of seismic stations. It decreases to approximately 1.2 km, while the seismic velocities vary in the range of 2.5–3.6 km s^{-1} (top/bottom). The different seismic structure of the sedimentary sections along the profile is also obvious in the 1-D velocity profiles (Figs 9a–c, 1–3).

For the residual crustal part of the model, the profile can be split (horizontally) into four segments S1–S4 for a better structural interpretation (see Figs 8 and 9a–d).

S1. The uniform, 80 km wide southern segment S1 extends up to the northern coastline of Spitsbergen Island. Seismic velocities in the top layer are 4.8–5.3 km s^{-1}, which thins to the north from 2.5 to 1.5 km (Fig. 9d, 4). As the profile is located at an acute angle to the strike of Forlandsundet Graben, this layer could represent the eroded and crushed cap of the eastern basement graben shoulder. Note that this layer of the velocity model is identical with that representing the Danskøya Basin (s.a.; Fig. 8). The boundary between both structures is realized by a large lateral velocity gradient in the model.

Below this layer the crust is composed of three units of similar velocity gradient (Fig. 9d, 5), subdivided by different seismic velocities and strong wide-angle reflections. The thickness of the upper layer decreases from 12 to 8.5 km towards the north. Seismic velocities range from 6.1 to 6.3 km s^{-1}. The middle unit, showing velocities of 6.4–6.6 km s^{-1} varies in thickness from 7 to 10 km and is characterized by a slight 2 km high uplift (200 km), which pushes through the lower layer down to the Moho level. The lowest layer, with a uniform thickness of ∼6 km and seismic velocities of 6.7–6.8 km s^{-1}, rests on the crust–mantle boundary. The total crustal thickness for this segment varies between 23–28 km.

S2. A narrow, 50–60 km wide segment S2 is situated below the shelf break and the southern Danskøya Basin. This trough-shaped segment narrows to 30 km at a depth of 18 km. It is characterized by decreased seismic velocities of 5.1–5.8 km s^{-1} in the upper crustal part (6–10 km) compared with the segment S1. These velocities belong most probably to Palaeozoic sediments (Figs 9c, 6). Seismic velocities increase constantly with a high gradient between 0.04 and 0.1 s^{-1} to a value of 6.5 km s^{-1} at a depth of 18 km (Fig. 9c, 7). Only weak reflections mark a boundary at 7–9 km depth. The lowest crustal layer exhibits the same seismic structure as observed in segment S1. The Moho is lifted up by approximately 4 km at the northern end of this segment so that the entire crustal thickness decreases to 21 km.

S3. Below the northern Danskøya Basin a 3–5 km thick layer with a constant seismic velocity of 6.0 km s^{-1} is observed. It is underlain by two units, which broaden with increasing depth. Seismic velocities at 9 km depth are approximately 6.7 km s^{-1} and increase gradually with a low gradient of 0.02 s^{-1} to 7.0 km s^{-1} at the crust–mantle boundary (Fig. 9b, 8). Wide-angle reflections constrain the 9 km boundary very well, while at greater depth no continuous reflector is observed. The highest crustal seismic velocities (7.0 km s^{-1}) along the entire profile are observed within segment S3.

S4. The northern, 60 km wide segment is only sampled by non-reversed shots, owing to the absence of stations north of 80.5°N.

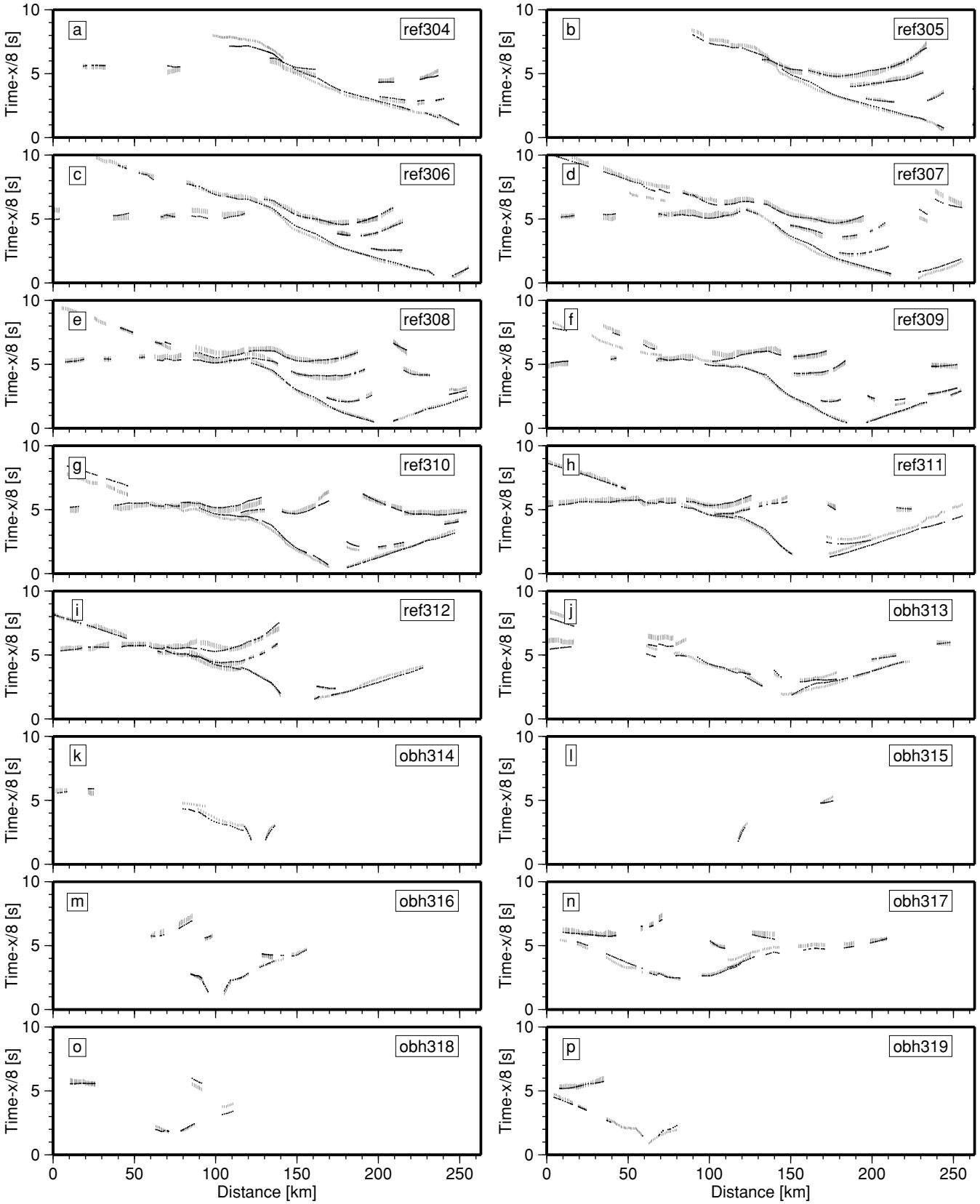

Figure 5. Observed and calculated *p*-wave arrivals for profile AWI-99300 (a–i: RefTek seismometer systems; j–p: ocean-bottom hydrophone systems). Grey errors bars indicate the assigned error to the picked traveltimes. The black lines show the traveltimes calculated using the final velocity model shown in Fig. 6.

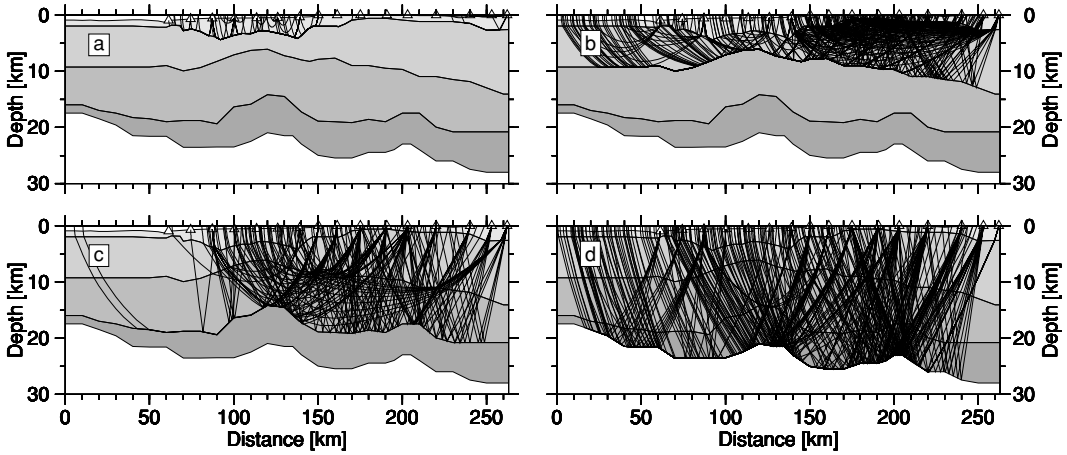

Figure 6. Raytracing for the four modelled crustal layers of profile AWI-99300 (every fifth ray). (a) Tertiary sediments. (b) Upper crust. (c) Middle crust. (d) Lower crust and mantle. Vertical exaggeration ×3.

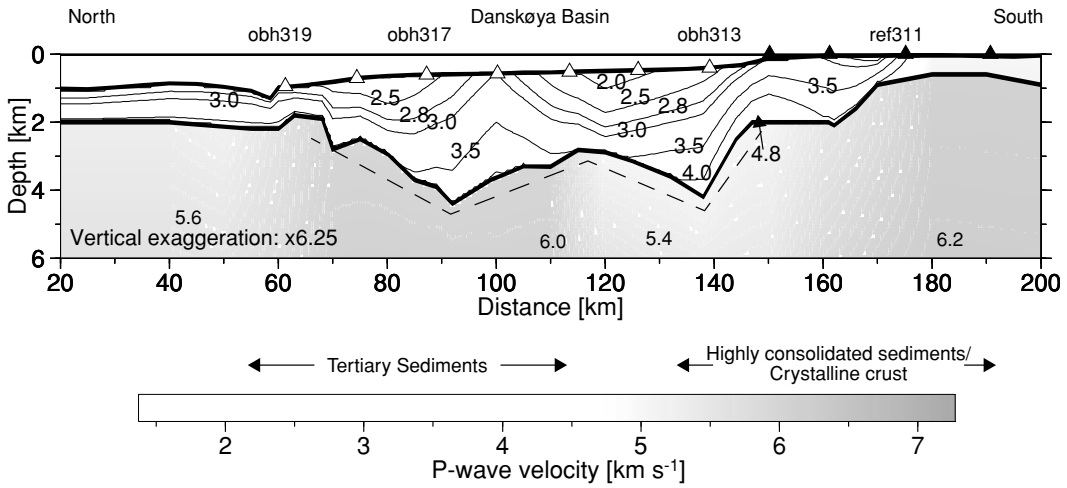

Figure 7. Final *p*-wave velocity model for the Tertiary sedimentary section of Danskøya Basin. Black and white triangles mark the positions of deployed seismic stations (RefTek-seismometer systems and ocean-bottom hydrophone systems). The dashed line marks the w-shaped surface of the basement below the Tertiary Danskøya Basin. For further explanations see Fig. 8.

Notwithstanding this, the seismic structure down to depths of 10 km and the entire crustal thickness are well constrained. Velocities at the top of the sub-Tertiary section of 5.3 km s^{-1} increase with a high gradient of 0.07 s^{-1} to 6.0 km s^{-1} at 9 km depth. As in segment S2 these velocities are suggested to be likely for Palaeozoic sediments (Fig. 9c, 6). The crust–mantle boundary is well constrained between 45–65 km. The curvature of reflected arrivals indicate moderate seismic velocities of 6.7 km s^{-1} at the Moho boundary. Station obh319 shows a weak reflection (Figs 4f and 5p), which supports the assumption that the crust–mantle boundary is shallowing north of 40 km. Fig. 5(p) shows the observed traveltimes for this reflection (10–40 km), which is best fitted with a shallowing Moho. Therefore, the final *p*-wave velocity model includes this shallowing, although this is in opposition to the results of gravity modelling (see below).

Upper mantle. Seismic velocities in the upper mantle are well constrained between 40 and 220 km along the profile, owing to numerous of p_n arrivals at the different seismic stations. The best fit of mantle refracted phases was reached at a velocity of 8.1 km s^{-1} along the profile. The phases were modelled as head waves, owing to the absence of a velocity gradient in these phases (Figs 9a–d, 9).

Resolution and uncertainty of the *p*-wave velocity model

The following procedures were applied to determine the quality of the final velocity model.

(1) The formal resolution of the velocity field parameters of the sedimentary and subsedimentary section was calculated by the inversion method of Zelt & Smith (1992). This quantitative approach is based on the relative number of rays that determine or assign the parametrization, i.e. the velocity–depth nodes. In the case of this study we determine only the resolution of the velocity nodes at a certain depth. Fig. 10 shows the resolution of the final model. Resolution values of 0.5 or greater are considered to be well resolved (Zelt & Smith 1992). The sedimentary section is well constrained in the region of Danskøya Basin (Fig. 10a). The lack of stations on the northernmost 50 km of the profile results in extremely low values for the sedimentary layer. The parametrization of this part of the model was kept fixed north of obh319 (61.3 km), as the velocity resolution is satisfied at this position. The seismic velocities of the shallow graben shoulder south of 180 km are not well resolved, but the resolution enhances to greater depths at the southern edge of the profile to values greater than 0.6.

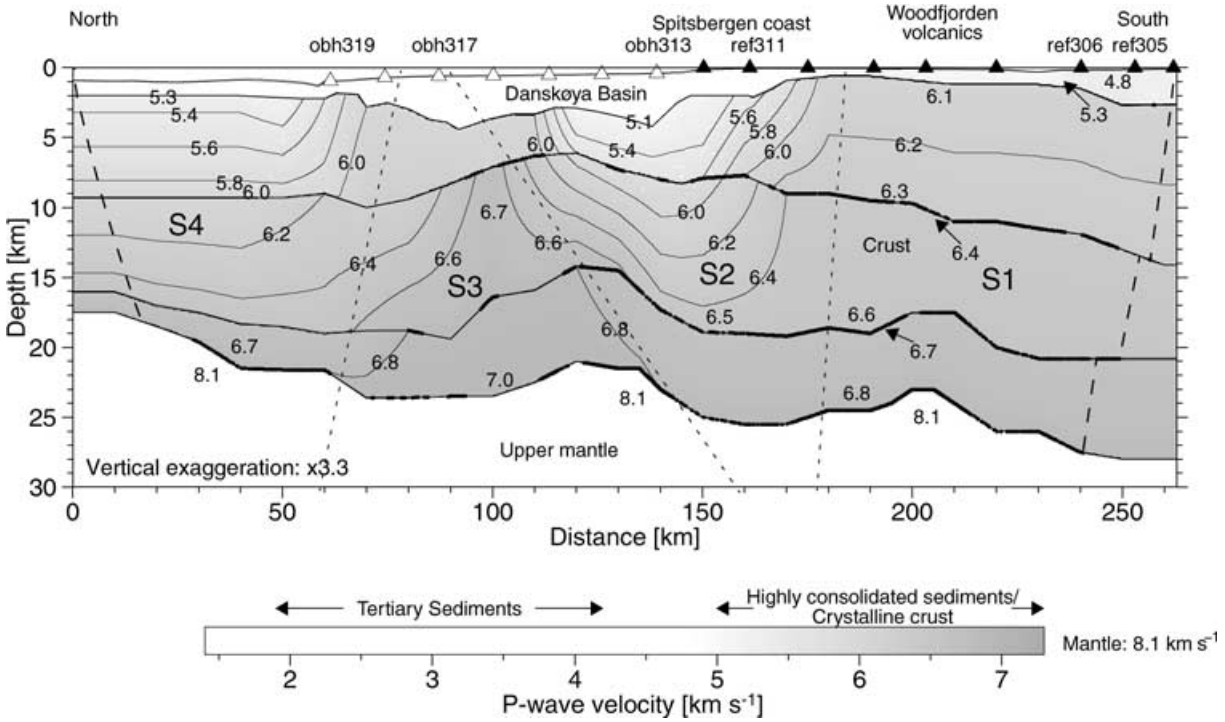

Figure 8. Final *p*-wave velocity model for profile AWI-99300. The grey shade and the contour lines (0.2 km s^{-1} interval from 5.4 to 6.8 km s^{-1}) show the crustal velocity field. Station locations along the profile are marked by white (obh) and black (ref) triangles. The dotted lines indicate the boundaries of the four crustal segments S1–S4 described in the text. The southern and northern maximum extents of penetrating rays are marked by thick dashed lines.

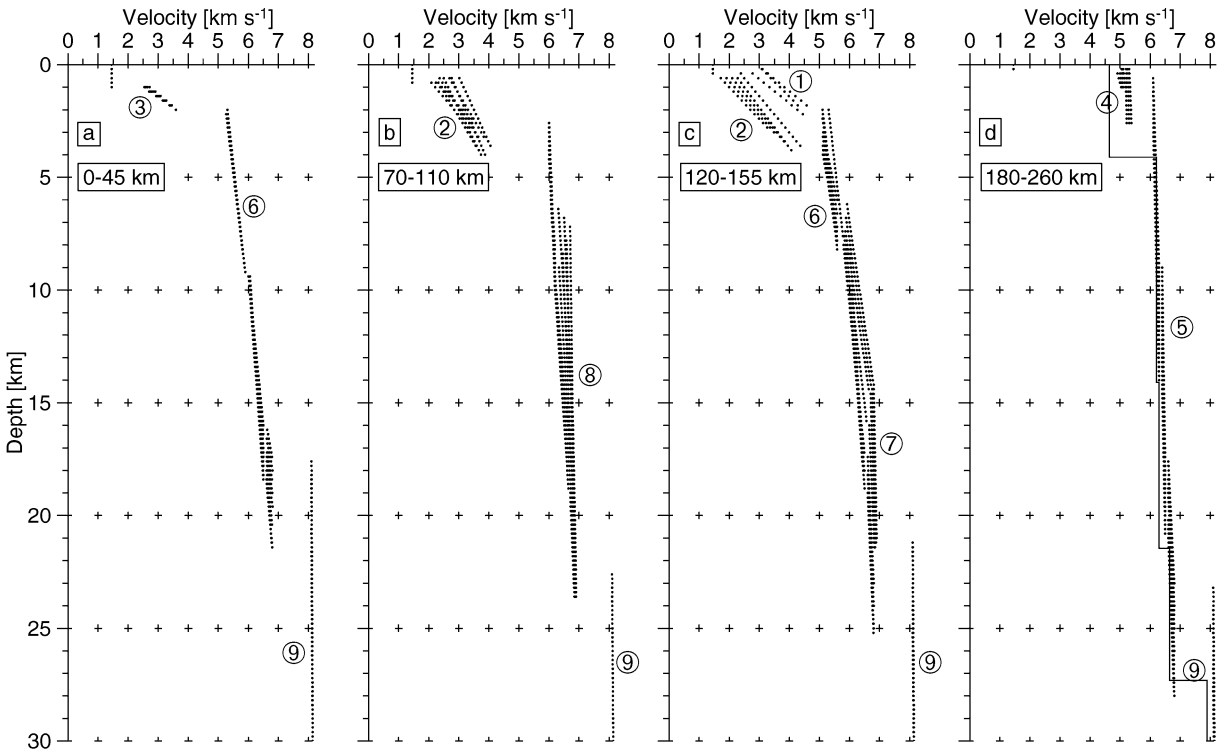

Figure 9. Seismic velocity–depth functions for profile AWI-99300, separated into the four crustal segments S1–S4 specified in the text: (a, S1) 0–45 km, (b, S2) 70–110 km, (c, S3) 120–155 km and (d, S4) 180–260 km, see also Fig. 6. Numbered circles: tertiary sediments: (1) inner shelf, (2) Danskøya Basin, (3) outer Yermak Plateau. Crustal sections: (4) Forlandsundet Graben shoulder, (5, 7, 8) continental crust, (6) Palaeozoic sediments (9) mantle. Additionally (d) shows the velocity–depth profile for northwestern Spitsbergen from Chan & Mitchell (1982) derived by traveltime and waveform analysis of seismic refraction data (solid line).

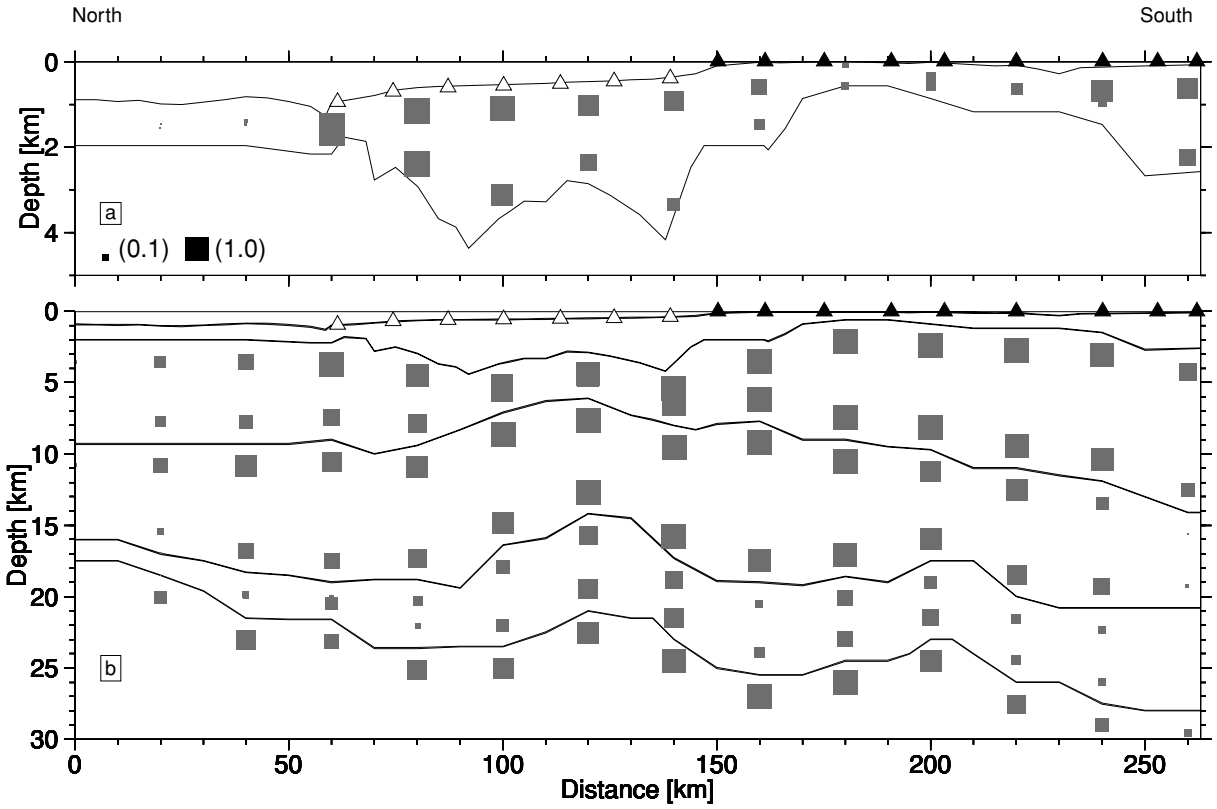

Figure 10. Resolution of the *p*-wave velocity field according to Zelt & Smith (1992) resampled to 20 km intervals along the profiles. The upper figure (a) shows values for the (Tertiary) sedimentary section (0–180 km) and the Forlandsundet Graben shoulder (180–263 km), the lower figure (b) for the underlying crust. The sizes of the grey squares are proportional to the quantified resolution. The black and white triangles mark the position of the seismic stations.

Generally, the resolution is satisfied for the preponderance of the subsedimentary section (50–220 km; Fig. 10b) as resolution values are mostly greater than 0.6. Owing to reduced ray coverage, the resolution decreases towards the northern flank of the model, where the values do not exceed 0.4. Resolution values for the deepest crustal layer decrease, owing to the small amount of direct velocity information from refracted energy traversing this layer. Upper-mantle velocities are well resolved, values greater than 0.6 are calculated.

(2) For the uncertainty of the depth level of the layer boundaries, which are mostly defined by wide-angle reflections (see Fig. 8, thick lines), the depth values of the individual reflectors were shifted both up and down until the calculated traveltime no longer fitted. The method depends strongly on the assigned size of the traveltime error (±100–200 ms) and the rms velocity of the penetrated crustal section. Determined uncertainties for the crustal reflectors are approximately 5–10 per cent of the absolute depth level. The error estimations are listed in Table 1.

(3) Depth-dependent uncertainties of the seismic velocities were derived by varying velocity values at certain depths, until the slope of a phase is significantly altered. Furthermore, the shifts in seismic velocity were performed within each modelled layer since the main parts of the traveltime branches do not fall outside the assigned errors of picked data. Although the technique is highly subjective, it gives a further evaluation criterion for the final velocity model. The determined uncertainties are listed in Table 2.

Table 1. Errors in depth level of the layer boundaries.

Boundary	Assigned error	Max. error in depth level	per cent of absolute depth
Upper/middle crust	±100 ms	±0.7 km	5.0–11.0
Middle/lower crust	±150 ms	±0.8 km	3.8–5.8
Lower crust/mantle	±200 ms	±0.8 km	2.9–4.5

Table 2. Errors in depth depended seismic velocity.

Layer	Velocity range	Max error in seismic velocity
Sedimentary section	2.0–4.8 km s^{-1}	±0.10 km s^{-1}
Upper/middle crust	5.1–6.3 km s^{-1}	±0.15 km s^{-1}
Middle/lower crust	5.9–6.7 km s^{-1}	±0.20 km s^{-1}
Lower crust	6.7–7.0 km s^{-1}	±0.25 km s^{-1}
Mantle	8.1 km s^{-1}	±0.10 km s^{-1}

4 GRAVITY MODELLING

Further constraints on the geological model of profile AWI-99300 are provided by 2-D gravity modelling, performed with LCT interpretation software (LCT user's guide 1998). The density of the water column was assumed to be 1.03 g cm^{-3}. For the densities of crystalline rocks the non-linear velocity–density relationship of Christensen & Mooney (1995) was used. Based on global studies this solution is suitable to calculate depth-dependent densities for crystal and peridotitic (mantle) rocks. All bodies were assumed to be 2-D, and have an infinite extent at each end of the density model.

The final *p*-wave velocity field was gridded and transformed to density. Blocks were digitized within an interval of 0.05 g cm^{-3} and used for the initial density model. For the main part of the profile, i.e. 40–260 km, this starting model fits the observed gravity well. After slightly shifting some boundaries within the

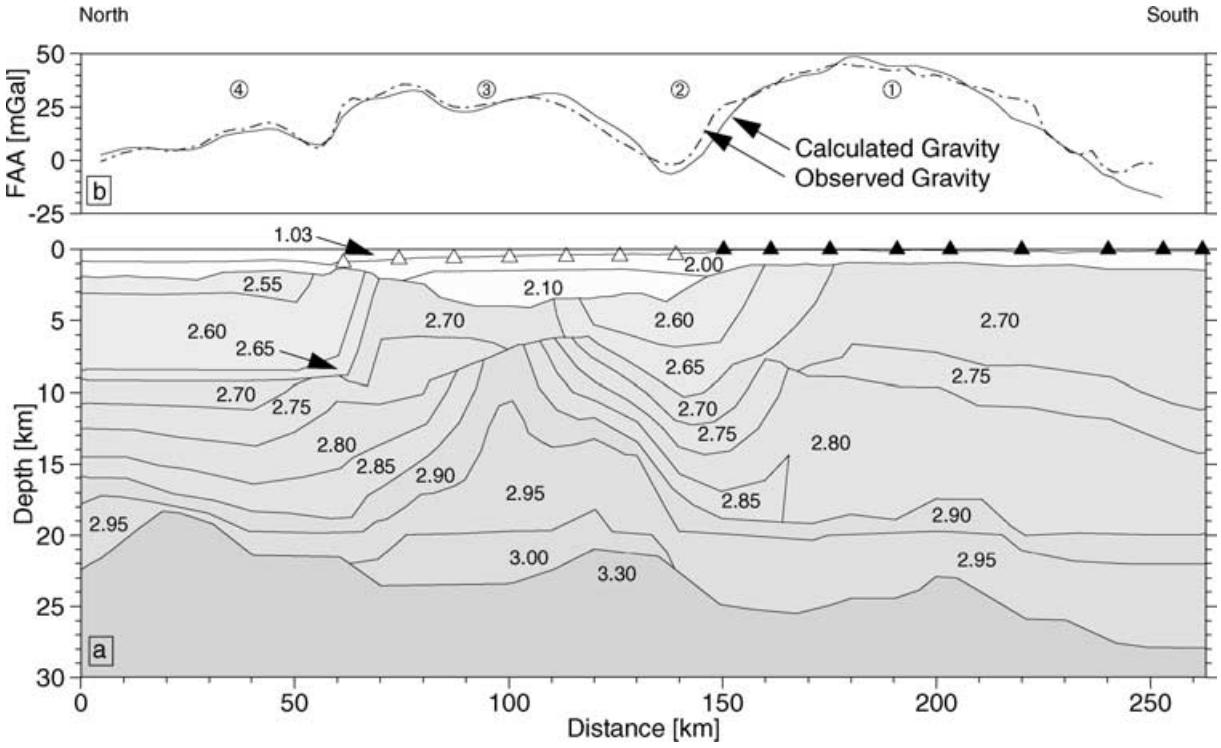

Figure 11. Final density model for profile AWI-99300 (a) with observed (dashed line) and modelled (solid line) free-air gravity. Density values (g cm^{-3}) are calculated by the non-linear regression of the velocity-density relationship of Christensen & Mooney (1995). Black and white triangles mark the positions of seismic station locations. At 0–40 km the fit to the observed gravity is achieved by an arbitrary 4 km downward shift of the crust–mantle boundary! This region is not well constrained by seismic refraction data, but the gravity modelling gives a reliable estimate for Moho topography.

determined depth uncertainties of the velocity model boundaries (Table 1), the resulting gravity field fits all observed anomalies well (Fig. 11).

For the northern part of the profile, i.e. 0–40 km, a coarse downward shift of 4 km in Moho level is necessary to fit the long-wavelength decrease of the observed gravity in the northward direction (Fig. 11). This is contrary to the final seismic refraction modelling result, in which reflection signals suggest possible shallowing of the Moho (Fig. 5p).

The observed gravity anomaly pattern (Fig. 11; 1–4) is explained by the following features of the final density model:

(1) the northward shallowing of mid-crustal rocks (2.75–2.80 g cm^{-3}) and slight shallowing of the Moho (160–260 km);

(2) the interplay of the deepening basement (Danskøya Basin) and low-density rocks (2.60–2.70 g cm^{-3}) in upper- and mid-crustal levels (120–160 km);

(3) the relatively dense rocks (2.85–2.95 g cm^{-3}) in mid-crustal levels (60–120 km);

(4) the low-density material (2.55–2.60 g cm^{-3}) in upper-crustal levels accompanied with a deepening Moho (0–60 km).

For the main part of the profile the density distribution confirms the crustal structures derived from seismic refraction modelling. At the northern end a downward correction in Moho depth is achieved.

5 GEOLOGICAL INTERPRETATION AND DISCUSSION

The following section is structured according to the segmentary structure of profile AWI-99300 (S1–S4; Figs 7 and 8). Fig. 12 summarizes the interpretation and shows a geological cross-section of northwestern Svalbard and the adjacent Yermak Plateau.

Segment S1

The segment S1 (Figs 8 and 12), located adjacent to the shoreline of northwestern Svalbard (Fig. 2) is built up of stretched continental crust, and shows similar thicknesses to those below the outer Isfjorden (e.g. Sellevoll *et al.* 1991; Czuba *et al.* 1999). Compared with the results of Chan & Mitchell (1982) we found a similar crustal structure, consisting of three lithological units, defined by seismic velocity (6.1–6.3, 6.4–6.6 and 6.7–6.8 km s^{-1}) and rock density (2.70–2.75, 2.80–2.90 and 2.95 g cm^{-3}). According to the work of Amundsen *et al.* (1987), on xenoliths from the Woodfjorden area (Fig. 2), and onshore geology structural information compiled by Harland (1997b), we propose the following rock types for the seismic units:

Upper unit (0–14 km depth). This unit consists of gneisses, migmatites and metasedimentary rocks, which are not covered by Palaeozoic sedimentary rocks as in the central part of northern Svalbard (Amundsen *et al.* 1987, Fig. 2). The final velocity model provides no evidence for a separation of less mafic granulites for this unit as proposed by Amundsen *et al.* (1987). The seismic data indicate a more or less homogeneous upper-crustal unit. Following the definition of Hecla Hoek-basement rocks (Harland 1997d), located to the east of the Billefjorden Fault Zone (Fig. 2) we do not use the term Hecla Hoek adopted by Amundsen *et al.* (1987) for our interpretation of the basement origin. Instead, we relate this upper unit to the unified basement province (terrane) west of the Raudfjorden Fault Zone (Fig. 2), which dips gently to the south,

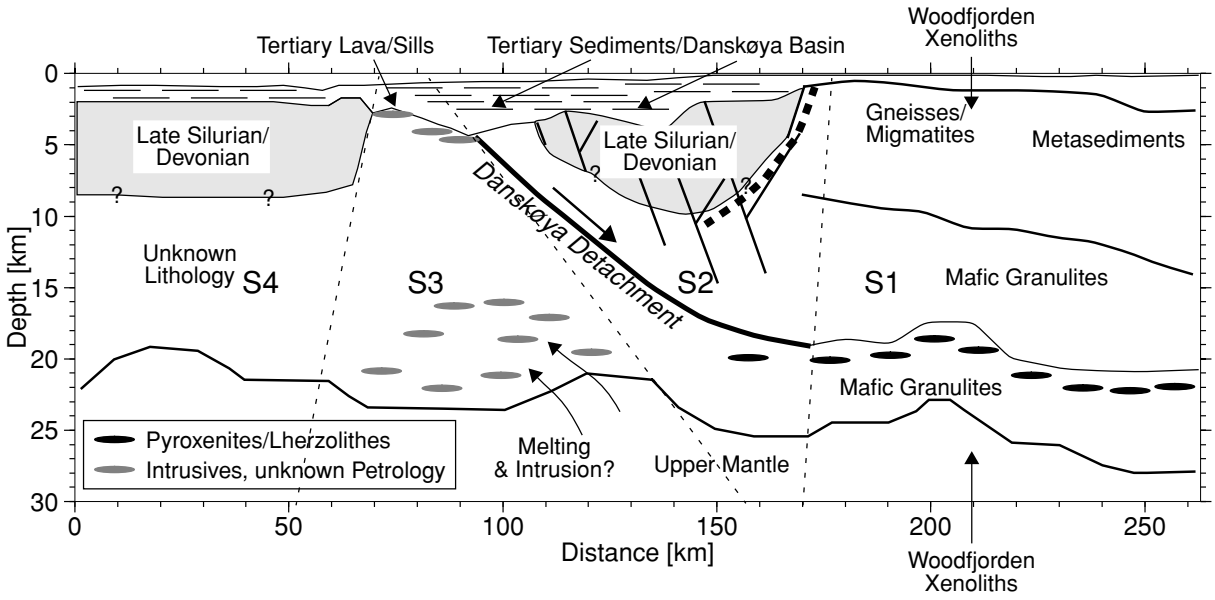

Figure 12. Final interpretation of the velocity model of profile AWI-99300. The dotted lines mark the boundaries of the four crustal segments S1–S4 as described in the text. Grey shaded regions marks the position of inferred Late Silurian/Devonian sedimentary basins. Between segments S2/S3 a thick black line marks the location of the proposed Cenozoic detachment fault. A possible north-dipping Caledonian Fault is marked by a dashed black line.

thus exposing deeper structural levels in the north. The southward dip of this unit is constrained by the observed seismic velocity structure, which shows a northward shallowing of the upper layer from 14 to 9.5 km depth along segment S1 (Fig. 8). The great variations in lithology throughout this basement province, from pre-dominantly metasediments in the south to gneisses and migmatites in the north (Hjelle 1979; Harland 1997b) is not visible in the smooth velocity structure (Fig. 8). Therefore, we also exclude further batholiths, as found further west in the northwestern Svalbard province along the seismic profile (i.e. Hornemantoppen Batholith).

Middle unit (14–21 km depth). At approximately 14 km depth Amundsen *et al.* (1987) define the boundary to mafic granulites. The seismic velocity of 6.4 km s^{-1} at depths of 10–14 km is rather lower than that for granulites at suitable p/T conditions observed in laboratory studies (approximately 6.7 km s^{-1}; Christensen & Mooney 1995). Instead, the observed seismic velocities of the mid-crustal unit are in better agreement with Palaeozoic orogenic areas, showing velocities of approximately 6.4 km s^{-1} (Holbrook *et al.* 1992). The earliest timing of Caledonian deformation found for the geological provinces west of the Raudfjorden Fault Zone (Fig. 2) is dated to the Mid-Silurian, within the Palaeozoic Caledonian orogeny (Harland 1997b). After Holbrook *et al.* (1992), likely compositions for the mid-crustal units are more felsic, e.g. granitic or granodioritic. The Woodfjorden xenoliths undoubtedly bear mafic two-pyroxene granulites, so we favour this composition for the mid-crustal unit, despite its slightly inconsistent velocity. We suggest that this deviation may point to a stronger tectonic overprinting, owing to the Cenozoic rifting processes.

Lower unit (21–28 km depth). According to Amundsen *et al.* (1987), the lower crust consists of mafic granulites, such as these of the middle crust, with interlayered mantle pyroxenites and/or lherzolites. The observed velocity range along the profile is consistent with the interpretation of Amundsen *et al.* (1987) that the lower crust consists most probably of mafic granulite rocks interbedded with pyroxenite lenses. From the seismic data it seems that these lenses occur at a depth level of 6.5 km above the crust–mantle boundary, which may reflect certain p/T conditions, forming a distinct lithological unit. At this level a strong reflector (6.6–6.7 km s^{-1}; Fig. 8) separates the lower-crustal portion along segment S1. Here the transition between the brittle and ductile crust is also expected. This may provide further good conditions for the accumulation of low amounts of mantle-derived pyroxenites/lherzolites.

Seismic velocities of 6.7–6.8 km s^{-1} at the crust–mantle boundary are characteristic for Palaeozoic orogenic regions. Furthermore, this is in agreement with velocities found below central Isfjorden, located 50–80 km to the southeast (Sellevoll *et al.* 1991).

A comparison with a seismic model for the lower-crustal structure of northwest Svalbard published by Czuba *et al.* (1999) shows obvious differences. The 10–15 km thick lower-crustal section of Czuba *et al.* (1999) showing seismic velocities of approximately 7.3 km s^{-1} is not confirmed by this study. The large discrepancies to Czuba's model (1999) may be a result of the experimental setup. The sparse shot–receiver distribution and non-reversed profiles were not able to provide non-ambiguous seismic data. Velocities greater than 7.2 km s^{-1} are typical for continental shield provinces (Holbrook *et al.* 1992) or passive (volcanic) margins influenced by mafic to ultramafic underplating (White & McKenzie 1989). We exclude magmatic underplating processes within segment S1, based on the observed lower seismic velocities. Furthermore, no evidence for excessive volcanism during breakup at 36 Ma has been found onshore. Our model combined with geology observations suggest it is more likely that a non-volcanic continental structure is present.

Segment S2/S3

Off the northwestern tip of Svalbard (Fig. 2) the upper and middle crustal velocities of segment S1 (Figs 8 and 12) are replaced by a zone of lower seismic velocities (>5.1 km s^{-1}) of segment S2. Further north, slightly higher velocities of 6.7–7.0 km s^{-1} in the middle and lower crust define segment S3.

The trough-like structure in segment S2, underlying the southern Danskøya Basin, shows seismic velocities of 5.1–6.0 km s^{-1}, which

we interpret as Palaeozoic, i.e. Late Silurian/Devonian sediments. We suggest, that the trough is bounded by faults, which may have been reactivated to facilitate Tertiary rifting. The base of the Palaeozoic sedimentary section in the trough is marked by velocities of 5.6–6.0 km s^{-1} at depths of 8–11 km. Thus the Palaeozoic sequence has a thickness of 4–7 km (Fig. 12), which is comparable to onshore observations on northwestern Svalbard (Harland 1997c). Younger post-Devonian sediments are not suggested here, since we assume similar sedimentary–erosional processes onshore and offshore for the northern central terrane.

According to onshore geological interpretations, subsiding Palaeozoic basins of the central terrane were the result of transtension tectonics since the Late Silurian (Friend *et al.* 1997). Pull-apart structures are interpreted as having developed in the vicinity of the Raudfjorden-, Hannabreen- and Breibogen Fault Zones, indicating Late Silurian/Devonian sedimentation in northern Svalbard. The occurrence of the Palaeozoic sequences to the north is poorly known, owing to the small number of offshore seismic investigations. (Eiken 1994a) suggests Devonian strata east of Danskøya Basin and south of the Moffen Fault (Fig. 2). Seismic velocities for Devonian strata on Svalbard are poorly known, although velocities of 4–6 km s^{-1} were recorded for younger Permian–Carboniferous sediments (Eiken 1994b). Fechner & Jokat (1996) and Schlindwein & Jokat (1999) found seismic velocities of 5.5 km s^{-1} and 5.3/5.7–6.0 km s^{-1} (surface/base) for Devonian sedimentary rocks to the east of the Caledonian orogen for the deeper Jameson Land Basin of the East Greenland Fjord Region, the structure of which is well known from onshore geology mapping.

Jokat (2000) mapped highly compacted Palaeozoic sedimentary rocks of a possible Caledonian foreland basin (Surlyk 1991, sedimentary deposits are not preserved onshore) below the Ob-Bank off northern Greenland showing seismic velocities of up to 5.8 km s^{-1} sediments. According to tectonic reconstructions and geological records (e.g. Harland & Wright 1979; Håkansson & Pedersen 1982) northern Greenland and Svalbard together occupied a wide depositional realm of the Caledonian orogen. The density model (Fig. 11) shows density values of 2.55–2.60 cm g^{-3} for the respective crustal section. In fact, this is a reasonable range for highly consolidated sedimentary rocks. It is therefore likely that the crust below the Danskøya Basin of segment S2 consists of Late Silurian/Devonian strata. The northern edge of this Palaeozoic basin is marked velocities ranging between 6.0 and 6.1 km s^{-1}. These seismic velocities are similar to those observed along segment S1 for the crystalline basement.

At depths of 20 km below the Palaeozoic basin of segment S2, seismic velocities are lower in comparison with the same level in segment S1. Further north seismic velocities along segment S3 increase to 6.6 km s^{-1}, indicating a pronounced lateral velocity variation at a depth of 20 km. Eiken (1993) emphasized the resemblance of the Danskøya Basin to a Tertiary pull-apart structure, owing to the fact that the bounding faults strike slightly oblique to the Hornsund Lineament (Fig. 2). Eiken (1993) proposed a simple shear rifting history as the origin for the Danskøya Basin. As a consequence of rifting, thin crust off the northwestern tip of Svalbard was suggested. Thinned crust cannot be confirmed by this study. However, the pronounced asymmetry in seismic velocity structure between the segments S2/S3 can be consistent with such a view. Following the detachment extension models of Lister *et al.* (1991), based on Wernicke's (1985) simple shear concept, the boundary between the segments S2/S3 might be interpreted as being a deep penetrating fault or detachment. According to Wernike's (1985) concept the upper plate (consisting here of the segments S1/S2) tends to brittle block-faulting, while the (segments S3/S4) crust–mantle boundary of the lower plate behaves in a ductile fashion forming a Moho uplift.

The zone of lower seismic velocities within the middle and lower parts of segment S2 (Fig. 8) may therefore be block-faulted and partly mylonitized, owing to extension. A faulted (acoustic) basement was found for the landward side of the southern Danskøya Basin (Eiken 1993). The low velocities in segment S2 at depths of 12–18 km can be attributed to ancient domino faults suspending and cracking the actual lithological structure of suggested mafic granulites (segment S1).

Stretching and uplift of the upper mantle can lead to its subsequent decompressive melting. The rising magma can crystallize at the base of the crust (underplating) or within its lower and middle parts, following zones of weakness (Lister *et al.* 1991). Thus, the lower parts of segment S3 may be interpreted as being slightly contaminated with mantle-derived melts, increasing the seismic velocity here (Lister *et al.* 1991). Eiken (1993) interprets strong and smooth reflections at the base of the sediments in the northern Danskøya Basin (below segment S3) as sills or lava flows; a further indicator of slight volcanic activity. Generally, the magmatism along segment S3 was essentially subdued, since the magnetic field pattern (Feden *et al.* 1979) appears to be rather smooth.

The seismic refraction data along profile AWI-99300 yield no consistent evidence for the suggested reflectivity of a mylonitic detachment or fault zone at the base of the Palaeozoic sedimentary section (Etheridge & Vernon 1983; Fountain *et al.* 1984). Here, the boundary between segments S2 and S3 shows no significant impedance contrast. The wavelength of seismic signals is ∼750 m at seismic velocities of 6 km s^{-1} and a frequency of 8 Hz. Thus, if the velocity distribution and the geometry of the segments S2 and S3 are caused by the presence of a detachment fault, a discrete mylonite zone on this plane must have a very low thickness of less than ∼190 m according to the formal vertical resolution. However, a gradual transition from the mylonite zone to the (undisturbed) surrounding rock units is probably more natural, resulting in an impedance contrast that is not sufficient.

Summarizing the discussion for the segments S2/S3 we conclude that a Late Silurian/Devonian basin exists within segment S2. The *p*-wave velocity range found for shore rocks deposited after the Caledonian orogeny is very similar to those we found. The strong asymmetry in crustal construction supports extensional detachment tectonics so it is possible that the segments are separated by a detachment fault. Regarding the pull-apart character of the Oligocene Danskøya Basin (Eiken 1993) we support models that require simple shear processes for the Mid-Cenozoic rifting.

The existence of a deeper seated Devonian Basin indicates that extensional movements took place during the Caledonian orogeny. Striking support is also given by recent geological mapping (Friend *et al.* 1997) at the Siktefjellet Strike-Slip Zone (Fig. 2), which discovered half-grabens in a pull-apart basin of Late Silurian/Early Devonian age. These grabens are related to strike-slip movements along the Raudfjorden Fault and the Breibogen Fault, and detachment tectonics between the brittle upper and ductile lower crust (Fig. 13a). A similar tectonic origin is considered for the formation of the Palaeozoic Basin below Danskøya Basin, which is located 50 km to the northwest (Fig. 13b). Thus, it is required that the Raudfjorden Fault (or a related major fault) extends further to the north to enable Palaeozoic half-graben formation below the Danskøya Basin. The subsequent Tertiary extension and the formation of the Danskøya Basin was accompanied by the reversal of the strike-slip motion from sinistral

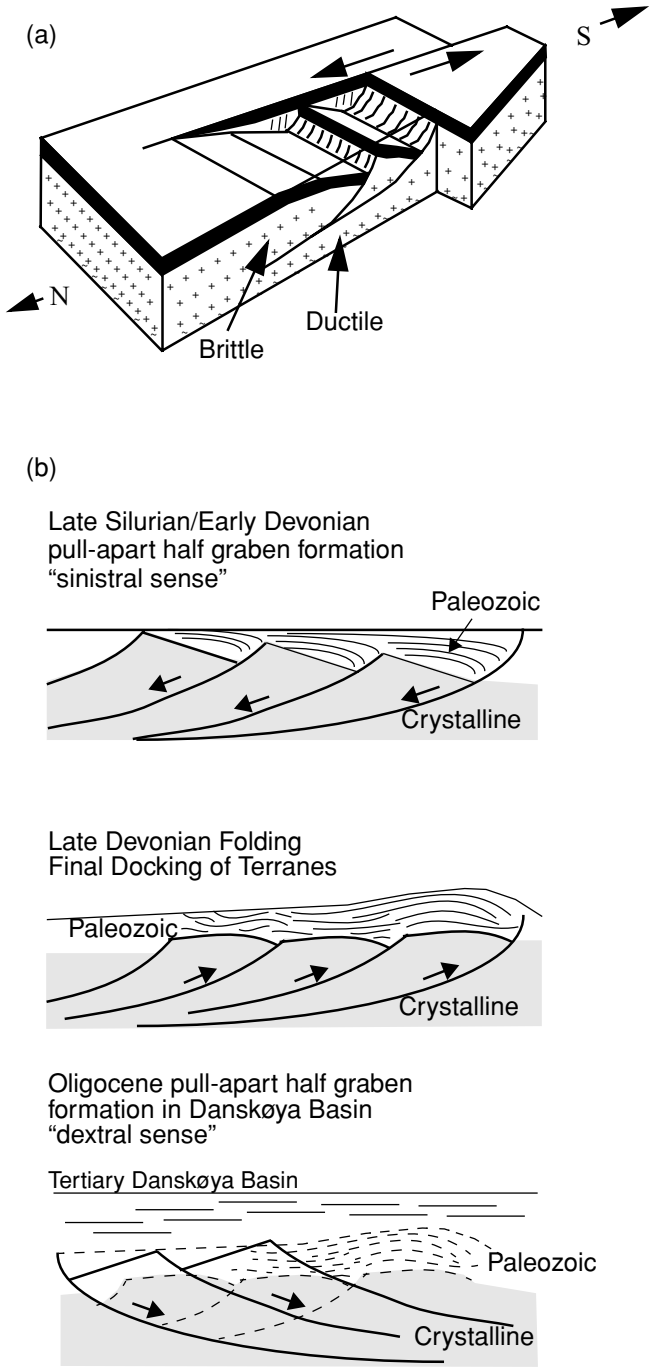

Figure 13. (a) Block diagram showing the principal growth of pull-apart half grabens in a sinistral strike-slip zone. This geometry is supposed for the depositional setting of the Devonian Siktefjellet Strike Slip Zone (Fig. 2; after Friend *et al.* 1997). The same tectonic is considered for the formation of the Palaeozoic Basin below Danskøya Basin, which is located 50 km to the northwest. (b) Schematic evolution of the Danskøya Basin crustal section (Palaeozoic to Cenozoic; Palaeozoic: after Friend *et al.* 1997).

(Caledonian terrane accretion) to dextral sense (Cenozoic breakup of Svalbard from northeast Greenland; Fig. 13b). It seems that Tertiary transtension occurred at a location with a Palaeozoic faulting history, which provided possible zones of weakness within the crust.

Segment S4

Compared with the velocity structure along segment S1, segment S4 (Figs 8 and 12) shows a similar crustal thickness derived from seismic and gravity modelling. Lower seismic velocities of 5.3–5.8 km s^{-1} are present within the upper-crustal section. Following the interpretation of Palaeozoic sediments in segment S2, we suggest the existence of post-Caledonian sediments here, north of the Danskøya Basin. The observed acoustic basement in seismic reflection data (approximately 2 s TWT; Eiken 1994c) may represent a sediment–sediment boundary. Assuming velocities up to 6.0 km s^{-1} for Palaeozoic sediments, the actual sediment–basement boundary may be located at depths of 8–10 km.

The final velocity model (Fig. 8) constrains a reflective boundary, separating velocities of 6.0 from 6.1 km s^{-1}. The latter velocity seems likely to be related to northern Svalbard crystalline rocks, as observed along segment S1 and confirmed by onshore geological observations. The thickness of the crystalline crust decreases to 10–14 km below the Devonian basin (Fig. 12). A lithological interpretation is difficult. The Svalbard central terrane of the Caledonian and Ellesmerian orogeny might extend as a spur northwest of Norskebanken (Fig. 2). Therefore, a similar lithology as found for the central terrane onshore might be expected.

The northern edge of profile AWI-99300 adjoins the southern H.U. Sverdrup Bank, the origin of which is the subject of speculation. Seismic refraction data from the H.U. Sverdrup Bank (Austegard 1982) revealed seismic velocities generally greater than 5 km s^{-1}. Eiken (1993, 1994d) interprets the H.U. Sverdrup Bank as a crystalline block, owing to its smooth aeromagnetic character (Feden *et al.* 1979) and dredged Precambrian gneisses (Jackson *et al.* 1984). Our deep seismic profile AWI-99300 provides no new evidence concerning the nature of the bank. The direct juxtaposition of a Devonian basin (segment S4) with the H.U. Sverdrup Bank may point to a Palaeozoic sedimentary origin for the uppermost section.

6 TECTONIC IMPLICATIONS

Following the interpretation and discussion of the resulting geological model of profile AWI-99300, two implications can be drawn. (1) The nature and magmatic history of the Yermak Plateau, with regard to the proposed Yermak Hotspot (Feden *et al.* 1979; Jackson *et al.* 1984), must be revised, because the observed crustal structure exhibits no evidence for plume activity. (2) The proposed Cenozoic simple shear processes entail an isostatic response on the lithosphere of northern Svalbard and the Yermak Plateau, and therefore uplift of the Svalbard region.

The nature and magmatic history of the Yermak Plateau

From Prins Karls Forland (Fig. 2) up to the northern edge of the profile AWI-99300 slightly thinned continental crust is present, showing a relatively constant crustal thickness. The southern section of the profile is associated with the basement province cropping out west of the Raudfjorden Fault on Svalbard (Fig. 2; Harland 1997b). It is part of the Svalbard central terrane in the north of the Kongsfjorden–Hansbreen Fault Zone (Fig. 2; Harland & Wright 1979). The Danskøya detachment fault separates this province from a further continental fragment, i.e. segment S4 that might also be related to the central terrane province. According to gravity field observations (Boebel 2000) stretched continental crust on the western Yermak Plateau is bounded by strong gravimetric anomalies

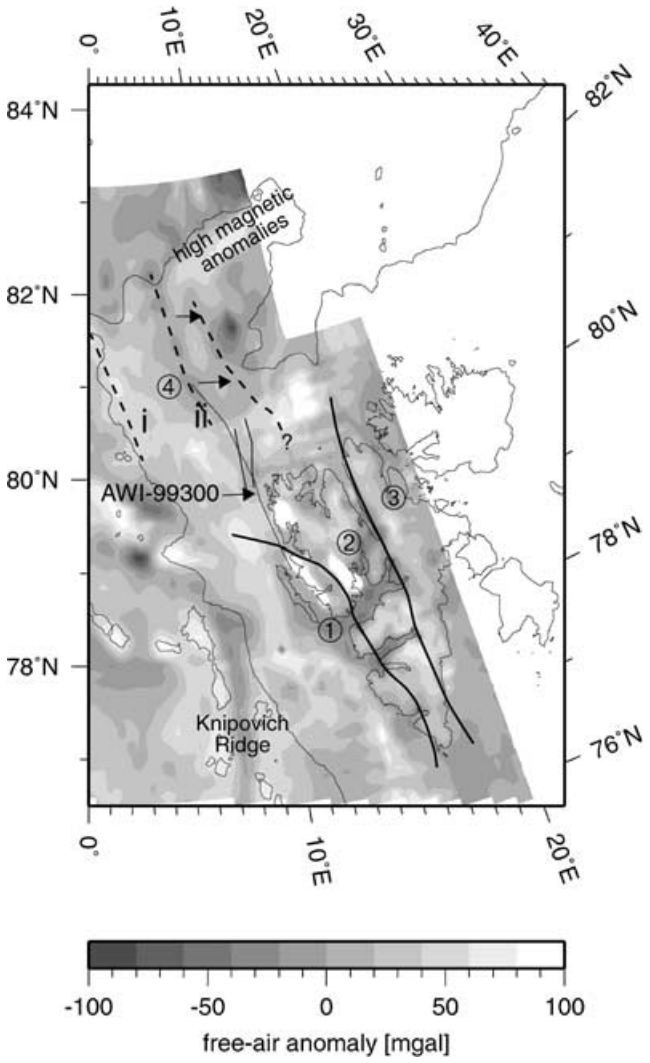

Figure 14. Free-air anomaly grid of Boebel (2000). Thick black lines on Svalbard separate the three proposed terranes ((1) western, (2) central, (3) eastern terrane). The gravity high anomaly i is suggested to express the western continent–ocean transition of a stretched continental fragment (4) (Boebel 2000). The gravity low (ii) indicates its proposed eastern boundary. Note, that profile AWI-99300 (thin line) is located to the east of anomaly (ii), so that the transition probably occurs further east (arrows). The continental fragment of the Yermak Plateau probably belongs to the central terrane of Svalbard. Zone of enhanced magnetic anomalies after Feden *et al.* (1979). Bathymetry: (IBCAO; Jakobsson *et al.* 2000, 2000 m-contour).

(see Fig. 14; i and ii). Most probably stretched continental crust reaches up to 82°N, separating the oceanic Fram Strait spreading system (anomaly i) from the oceanic Yermak Plateau province at 82°N (anomaly ii), the conjugate to the Morris Jesup Rise (Figs 1 and 14; Boebel 2000). Southward, the eastern anomaly (ii) intersects with the profile where stretched continental crust is present. We conclude, that anomaly (ii) reflects the summit of a stretched fragment rather than the eastern boundary to an oceanic province south of 82°N as proposed by Boebel (2000). The actual continent–ocean boundary occurs probably 30 km further east (Fig. 14).

Up to 81°N, the observed crustal structure along profile AWI-99300 provides no evidence for increased magmatic activity, owing to the presence of the Yermak Hot Spot (Feden *et al.* 1979; Jackson *et al.* 1984). Plume-related features such as volcanic wedges, numerous intrusions or underplating as found for North Atlantic continental margins (e.g. Barton & White 1997) are missing here. For the case of the North Atlantic the influence of the mantle plume extends up to 2000 km distance from its head. The distance from the northern tip of profile AWI-99300 to the strong magnetic anomaly pattern in the northeast (Fig. 14), which was interpreted as a result of plume activity on the Yermak Plateau (Feden *et al.* 1979) is just 150 km. A stretching factor of $\beta = 1.2$–1.6 is calculated between the mean crustal thickness of the central terrane (35 km; Sellevoll *et al.* 1991) and the observed values along profile AWI-99300 (21–28 km). Applying these factors to the distance between the northern termination of profile AWI-99300 and the high magnetic anomalies shortens to 100 km.

Furthermore, it has to be considered that western Svalbard adjoins the Spitsbergen Shear Zone, which marks the plate boundary between Svalbard and Greenland in Oligocene times (Crane *et al.* 1991). Lithospheric thinning is suggested along the fracture (Crane *et al.* 1991), which would therefore lead to channelling of the plume through this zone towards the south (Thompson & Gibson 1991; Saunders *et al.* 1992). Decompressive melting caused by a lesser lithospheric load would provide a simple path for distribution of large amounts of melts associated with the hot mantle plume. Further north–south-striking major faults on the Svalbard Archipelago (Fig. 2) might also control the plume evolution. Although good boundary conditions are given only a slight amount of intrusives is observed below the central and southern Yermak Plateau. Therefore, the intrusives below the detachment fault in the lower crust, seem to be more consistent with decompressive melting (Lister *et al.* 1991) as a consequence of the extensional processes and subsequent slight uplift of the crust–mantle boundary.

The temperature of the asthenosphere determined on Neogene volcanics of the Woodfjorden area (Fig. 2) is 1350 °C, slightly above that of normal asthenosphere (Vågnes & Amundsen 1993). This is rather low, compared with temperature anomalies reported from other hotspots (+200–300°C; Vågnes & Amundsen 1993). It seems more likely that the Oligocene volcanic activity was a local phenomenon situated and restricted to the northeastern Yermak Plateau (Figs 14 and 15) along an ancient section of the Gakkel Ridge. Therefore, we prefer a non-volcanic continental margin evolution for the northwest Svalbard and Yermak Plateau continental margins investigated here.

Consequently, local volcanic activities further south, i.e. northern Danskøya Basin and Woodfjorden volcanics, appear to be not linked to any mantle plume influences. More likely they seem to also be related to the extensional lithospheric shear processes below the Danskøya Basin during the Cenozoic, destroying the internal structure of the continental crust and providing paths for mantle-derived melts.

Cenozoic tectonics between Greenland and Svalbard and subsequent uplift

Since Late Cretaceous times the main transcurrence/transtension fault system between Svalbard and Greenland, migrated continuously eastwards (Håkansson & Pedersen 1982; Crane *et al.* 1991). First movements started at the Trolle–Land Fault system, while later a jump to the Hornsund Lineament occurred (Fig. 15). The transfer movements were not limited to a single fault, but were rather spread over a broader region, so that local pull-apart basins developed (e.g. predestination of the Molloy Ridge (Crane *et al.* 1991), Trolle–Land Fault Zone, Håkansson & Pedersen (1982)). The

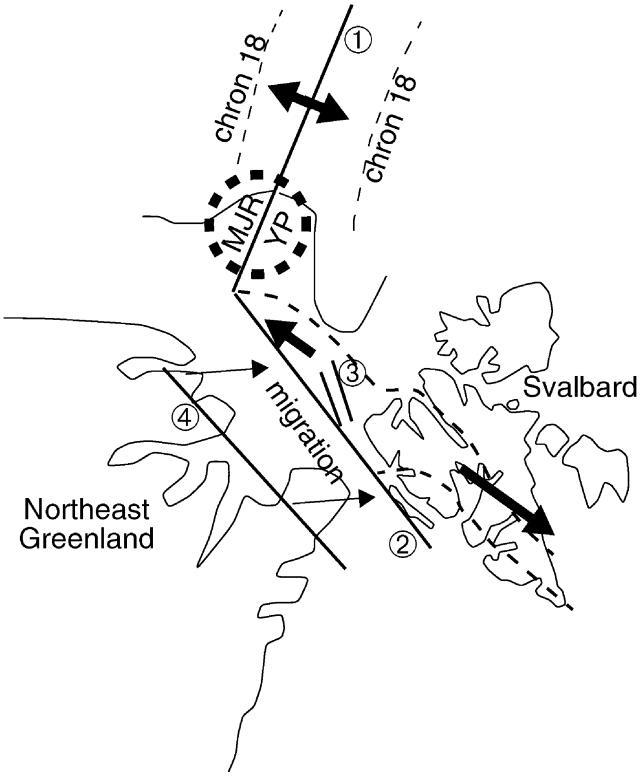

Figure 15. Oligocene schematic plate tectonic configuration (36 Ma) after Boebel (2000) including a boundary of the northern continuation of the Svalbard central terrane resulting from this study. Thin dashed lines along the Gakkel Ridge mark the position of chron 18. In pre-Oligocene times northeast Greenland, Svalbard and the juvenile Gakkel Ridge (1) adjoined a triple junction (RFF- system). From 36 Ma onwards, Gakkel Ridge spreading and transtensional movements along the Hornsund Lineament (2; thick arrows) caused the breakup of Svalbard from northeast Greenland. The Danskøya Basin (3) and a detachment below developed (or was reactivated). Later, at 20 Ma, seafloor spreading started in the Fram Strait, to finally connect the North Atlantic MOR system (Mohns Ridge–Knipovich Ridge; Fig. 1) with the Arctic Gakkel Ridge. Local volcanism formed the northeastern Yermak Plateau (YP; position of enhanced magnetic anomalies) and the Morris Jesup Rise (MJR; thick dashed circle) during Oligocene. The actual constructions of these geological features (YP and MJR) are still subject of speculations. Broader plume activity that formed a large volcanic plateau consisting of thickened oceanic crust is excluded, since the continental spur of the Svalbard central terrane exhibits no evidence for higher magmatic activity. The transform fault systems between Greenland and Svalbard moved continuously eastwards (e.g. Trolle-land Fault Zone (4) to Hornsund Lineament) from Late Cretaceous onwards. Fault systems commonly feature pull-apart structures. The most recent of these is the Danskøya Basin on the southern Yermak Plateau. Thicker dashed lines on Svalbard and Yermak Plateau indicate terrane boundaries.

development of the Danskøya Basin and the detachment tectonics fit with this interpretation, since it defines the eastern termination of migrating strike-slip tectonics. Eiken (1993) mentioned the pull-apart character of the Danskøya Basin, although its precise shape is unknown. The geological interpretation of the final velocity model (Fig. 12) supports this interpretation.

The continental Yermak Plateau fragment underwent extension from Oligocene onwards, so that a juvenile rift structure developed. Svalbard and the surrounding Barents Sea region experienced uplift and erosion during the Cenozoic, as shown by geological records and model calculations (Doré & Jensen 1996). A first uplift phase is supposed to have a tectonic origin, probably occurring in several episodes throughout the Cenozoic. A second phase is associated with the rebound from ice-sheets of the great glaciations of the Pliocene and Pleistocene (Doré & Jensen 1996). Total erosion of 3000 m is supposed for the southwestern Svalbard region, mainly caused by glacial erosion (Dimakis *et al.* 1998). For the marginal rift flanks of the Barents Sea (i.e. Senja Fracture Zone–Western Svalbard and Nordaustlandet–Franz Josef Land; Fig. 1) only 500–100 m of uplift is related to rifting, breakup and subsequent opening of the adjacent ocean basin. This is most probably owing to: (1) a heat-transfer-defining temperature distribution and therefore flexural rigidity of the lithosphere and (2) lithospheric shear mechanical flexure during breakup, respectively, (Dimakis *et al.* 1998). Regarding the detachment models of Lister *et al.* (1991), we suggest an additional local component for the southern Yermak Plateau that interacts with rift-induced tectonic uplift along the western rim of the Barents Sea. Mid-crustal detachments and crustal thinning (Lister *et al.* 1991) can lead to uplift during the rift phase followed by a post-rift subsidence phase. Model calculations with a detachment fault at 15 km depth and an initial crustal thickness of 35 km result in a maximum net uplift of 600 m (Lister *et al.* 1991). Since a full rifting phase was not completed at the southern Yermak Plateau, the maximum amount cannot be expected. With a stretching factor of $\beta = 1.2$–1.5 a net uplift of up to 300 m is possible (Lister *et al.* 1991) superimposed on broader tectonic events.

7 CONCLUSIONS

Transtensional tectonics during the breakup of Svalbard and Greenland thinned the crust from 35 km below inner Svalbard to 18–28 km as observed along the profile. The deep structure of the southern section of the profile can be related to the basement province west of the Raudfjorden Fault building up the central terrane of Svalbard. The character of the stretched continental crust remains similar on the northern Yermak Plateau, but the actual lithology of the middle and lower crust remains speculative.

North of the Svalbard coastline the velocity structure supports the existence of a detachment fault, although the fault plane is not resolved in the seismic data itself. Above this, the Tertiary Danskøya Basin is underlain by a Palaeozoic sedimentary basin, of suggested Late Silurian/Devonian age. The Palaeozoic sedimentary origin of that basin is constrained by low seismic velocities of 5.1–5.8 km s^{-1}, which are typical for Devonian rocks of Greenland and Svalbard. Palaeozoic sedimentary rocks may also occur in the upper section (6 km) between the H.U. Sverdrup Bank and the Danskøya Basin. The onset of extension in the Danskøya Basin above the detachment was in the Oligocene, while its duration is speculative. Owing to the obvious asymmetric construction, simple shear rifting is supposed. This might have driven an uplift of maximum 300 m in the Cenozoic.

The final velocity model reveals no evidence for a large-scale influence and magmatism of a suggested hotspot during the breakup of Svalbard from northern Greenland (Yermak Hot Spot). The boundary conditions for a widespread distribution of mantle-derived melts are generally given since thin lithosphere can control the evolution of the plume along the major fractures and would provide ideal paths.

We propose that the observed crustal structure is typical for the entire western plateau up to 82°N, which is thus a stretched spur of the continental central terrane of Svalbard.

The volcanism that created the northeastern Yermak Plateau and the Morris Jesup Rise seems to have been local and short-lived, and is therefore unrelated to mantle plume activity as proposed for the

North Atlantic margins. Therefore, non-volcanic continental margins for northern and western Svalbard may be expected. Known volcanic events further south are, according to our interpretation, related to melt generation caused by simple shear tectonics combined with a slightly increased asthenospheric temperature.

ACKNOWLEDGMENTS

We are grateful for the excellent support from the captains and crews of RV Polarstern and RS El Tanin. We give a special thanks to our Polish colleagues A. Guterch, W. Czuba and P. Sroda, who supported measurements during the cruise.

REFERENCES

Amundsen, H.E.F., Griffin, W.L. & O'Reilly, S.Y., 1987. The lower crust and upper mantle beneath northwestern Spitsbergen: evidence from xenoliths and geophysics, *Tectonophysics,* **139**, 169–185.

Austegard, A., 1982. *Velocity Analysis of Sonobuoy Data from the Northern Svalbard Margin,* Seismol. Obs. Scientific Report, 9, University of Bergen, Bergen.

Austegard, A. & Sundvor, E., 1991. *The Svalbard Continental Margin: Crustal Structure from Analysis of Deep Seismic Profiles and Gravity,* Seismo-Series, 53, University of Bergen, Bergen.

Barton, A.J. & White, R.S., 1997. Crustal structure of Edoras Bank continental margin and mantle thermal anomalies beneath the North Atlantic, *J. geophys. Res.,* **102**, 3109–3129.

Boebel, T., 2000. *Airborne Topography and Gravimetry: System and Application to Fram Strait, Svalbard and Northeast Greeland,* Reports on Polar Research, 366, Alfred Wegener Institute for Polar and Marine Research, Bremerhaven.

Chan, W.W. & Mitchell, B.J., 1982. Synthetic seismogram and surface wave contrains on crustal models of Spitsbergen, *Tectonophysics,* **89**, 51–76.

Christensen, N.I. & Mooney, W.D., 1995. Seismic velocity structure and composition of the continental crust: a global view, *J. geophys. Res.,* **100**, 9761–9788.

Crane, K., Sundvor, E., Buck, R. & Martinez, F., 1991. Rifting in the Northern Norwegian–Greenland sea: thermal tests of asymmetric spreading, *J. geophys. Res.,* **96**, 14 529–14 550.

Czuba, W., Grad, M. & Guterch, A., 1999. Crustal structure of north-western Spitsbergen from DSS measurements, *Polish Polar Res.,* **20**, 131–148.

Dimakis, P., Braathen, B.I., Faleide, J.I., Elverhøi, A. & Gudlaugsson, S.T., 1998. Cenozoic erosion and the preglacial uplift of the Svalbard–Barents Sea region, *Tectonophysics,* **300**, 311–327.

Doré, A.G. & Jensen, L.N., 1996. The impact of Late Cenozoic uplift and erosion on hydrocarbon exploration: offshore Norway and other uplifted basins, *Global planet. Change,* **12**, 415–436.

Eiken, O., 1993. An outline of the northwestern Svalbard continenal margin, in *Arctic Petroleum Potential,* pp. 619–629, eds Vorren, T.O., Bergsager, E., Dahl-Stamnes, Ø.A., Holter, E., Johansen, B., Lie, E. & Lund, T.B., NPF Special Publication, 2, Elsevier, Amsterdam.

Eiken, O., 1994a. Southern Yermak Plateau—northern coast of Spitsbergen, in *Seismic Atlas of Western Svalbard—a Selection of Regional Seismic Transects,* pp. 25–26, ed. Eiken, O., Norsk Polarinstitutt Meddelelser, 130, Norsk Polarinstitutt, Oslo.

Eiken, O., 1994b. Aspects of the seismic method, in *Seismic Atlas of Western Svalbard—a Selection of Regional Seismic Transects,* pp. 59–63, ed. Eiken, O., Norsk Polarinstitutt Meddelelser, 130, Norsk Polarinstitutt, Oslo.

Eiken, O., 1994c. Yermak Plateau—Nansen Basin, in *Seismic Atlas of Western Svalbard—a Selection of Regional Seismic Transects,* pp. 27–28, ed. Eiken, O., Norsk Polarinstitutt Meddelelser, 130, Norsk Polarinstitutt, Oslo.

Eiken, O., 1994d. Southern Yermak Plateau, in *Seismic Atlas of Western Svalbard—a Selection of Regional Seismic Transects,* p. 28, ed. Eiken, O., Norsk Polarinstitutt Meddelelser, 130, Norsk Polarinstitutt, Oslo.

Eiken, O. & Austegard, A., 1987. The Tertiary orogenic belt of West-Spitsbergen: Seismic expressions of the offshore sedimentary basins, *Norsk Geologisk Tidsskrift,* **67**, 383–394.

Eldholm, O., Faleide, J.I. & Myhre, A.M., 1987. Continent–ocean transition at the western Barents Sea/Svalbard continental margin, *Geology,* **15**, 1118–1122.

Etheridge, M.A. & Vernon, R.H., 1983. Comment on "Seismic velocity and anisotropy in mylonites and the reflectivity of deep crustal fault zones", *Geology,* **11**, 487–489.

Fechner, N. & Jokat, W., 1996. Seismic refraction investigations on the crustal structure of the western Jameson Land Basin, East Greenland, *J. geophys. Res.,* **101**, 15 867–15 881.

Feden, R.H., Vogt, P.R. & Fleming, H.S., 1979. Magnetic and bathymetric evidence for the 'Yermak Hot Spot' northwest of Svalbard in the Arctic Basin, *Earth planet. Sci. Lett.,* **44**, 18–38.

Forsberg, R., 1984. *A Study of Terrain Reductions, Density Anomalies and Geophysical Inversion Methods in Gravity Field Modelling,* Reports of the Department of Geodetic Science and Surveying, 355, Ohio State University, Columbus, Ohio.

Fountain, D.M., Hurich, C.A. & Smithson, S.B., 1984. Seismic reflectivity of mylonite zones in the crust, *Geology,* **12**, 195–198.

Friend, P.F., Harland, W.B., Rogers, D.A., Snape, I. & Thornley, S., 1997. Late Silurian and Early Devonian stratigraphy and probable strike-slip tectonics in northwestern Spitsbergen, *Geol. Mag.,* **134**, 459–479.

Geißler, W.H., 2001. Marine seismische Untersuchungen am nordlichen Kontinentalrand von Svalbard (Spitzbergen), *Diploma thesis,* Institute for Geophysics, Freiberg University of Mining and Technology, Freiberg, unpublished.

Guterch, A., Pajchel, J., Perchuc, E., Kowalski, J., Duda, S., Komber, G., Bojdys G. & Sellevoll, M.A., 1978. Seismic reconnaissance measurement on the crustal structure in the Spitsbergen Region 1976, University of Bergen Seismological Observatory, Bergen.

Håkansson, E. & Pedersen, S.A.S., 1982. Late Paleozoic to Tertiary tectonic evolution of the continental margin in North Greeland, in Arctic Geology and Geophysics, pp. 331–348, eds Embry, A.F. & Balkwill, H.R., Memoirs of the Canadian Society of Petroleum Geologists, 8.

Harland, W.B., 1997a. Svalbard's geological frame, in *The Geology of Svalbard,* pp. 23–44, Geological Survey Memoir, 17, The Geological Society, London.

Harland, W.B., 1997b. Northwestern Spitsbergen (with a contribution with Doubleday, P.A.), in *The Geology of Svalbard,* pp. 132–153, Geological Survey Memoir, 17, The Geological Society, London.

Harland, W.B., 1997c. Devonian History, in *The Geology of Svalbard,* pp. 289–309, Geological Survey Memoir, 17, The Geological Society, London.

Harland, W.B., 1997d. Northeastern Spitsbergen, in *The Geology of Svalbard,* pp. 110–131, Geological Survey Memoir, 17, The Geological Society, London.

Harland, W.B. & Wright, N.J.R., 1979. Alternative hypothesis for the pre-Carboniferous evolution of Svalbard, *Norsk Polarinstitutt Skrifter,* **167**, 89–117.

Hellebrand, E., 2000. Petrology, in *The Expedition ARKTIS-XV/2 of "Polarstern" in 1999,* pp. 59–70, ed. Jokat, W., Reports on Polar Research, 368, Alfred Wegener Institute for Polar and Marine Research, Bremerhaven.

Hjelle, A., 1979. Aspects of the geology of northwest Spitsbergen, *Norsk Polarinstitutt Skrifter,* **167**, 37–62.

Holbrook, W.S., Mooney, W.D. & Christensen, N.I., 1992. The seismic velocity structure of the deep continental crust, in *Continental Lower Crust,* pp. 1–43, eds Fountain, D.M., Arculus, R. & Kay, R.W., Developments in Geotectonics, 23, Elsevier, Amsterdam.

Jackson, H.R., Johnson, G.L., Sundvor, E. & Myhre, A.M., 1984. The Yermak Plateau: formed at a triple junction, *J. geophys. Res.,* **89**, 3223–3232.

Jakobsson, M., Cherkis, N.Z., Woodward, J., Macnab, R. & Coakley, 2000. New grid of Arctic bathymetry aids scientists and mapmakers, *EOS, Trans. Am. geophys. Un.,* **81**, 89, 93, 96.

Jokat, W., 2000. The Sediment Distribution below the North Greenland Continental Margin and the adjacent Lena Trough, *Polarforschung,* **68**, 71–82.

Kristoffersen, Y., 1990a. On the tectonic evolution and the paleoceanographic significance of the Fram Strait Gateway, in *Geological History of the Polar Oceans: Arctic Versus Antarctic,* pp. 63–76, eds Bleil, U. & Thiede, J., Kluwer, Amsterdam.

Kristoffersen, Y., 1990b. Eurasia Basin, in *The Artic Ocean region,* pp. 365–378, eds Grantz, A., Johnson, L. & Sweeney, J.F., The Geology of North America, Vol. L, Geological Society of America, Boulder, CO.

Lawver, L.A., Muller, R.D., Srivastava, S.P. & Roest, W., 1990. The opening of the Artic Ocean, in *Geological History of the Polar Oceans: Arctic Versus Antarctic,* pp. 29–62, eds Bleil, U. & Thiede, J., Kluwer, Amsterdam.

LCT user's guide, 1998. Houston.

Lister, G.S., Etheridge, M.A. & Symonds, P.A., 1991. Detachment models for the formation of passive continental margins, *Tectonics,* **10**, 1038–1064.

Müller, R.D. & Spielhagen, R.F., 1990. Evolution of the Central Tertiary Basin of Spitsbergen: towards a synthesis of sediment and plate tectonic history, *Palaeogeog. Palaeoclimat. Palaeoecol.,* **80**, 153–172.

Myhre, A.M. & Eldholm, O., 1988. The Western Svalbard margin (74°–80°N), *Marine Petroleum Geol.,* **5**, 143–156.

Posewang, J. & Mienert, J., 1999. High-resolution seismic studies of gas hydrates west of Svalbard, *Geo-Marine Lett.,* **19**, 150–156.

Saunders, A.D., Storey, M., Kent, R.W. & Norry, M.J., 1992. Consequences of plume-lithosphere interactions, in *Magmatism and the Causes of Continental Break-up,* pp. 41–60, eds Storey, B.C., Alabaster, T. & Pankhurst, R.J., Geol. Soc. Spec. Pub., 68, The Geological Society London, London.

Schlindwein, V. & Jokat, W., 1999. Structure and evolution of the continental crust of northern east Greenland from integrated geophysical studies, *J. geophys. Res.,* **104**, 15 227–15 245.

Sellevoll, M.A., Duda, S.J., Guterch, A., Pajchel, J., Perchus, E. & Thyssen, F., 1991. Crustal structure in the Svalbard region from seismic measurements, *Tectonophysics,* **189**, 55–71.

Skogseid, J., Planke, S., Faleide, J.I., Pedersen, T., Eldholm, O. & Neverdal, F., 2000. NE Atlantic continental rifting and volcanic margin formation, in *Dynamics of the Norwegian Margin,* pp. 295–326, ed. Nøttvedt, A., Geol. Soc. Spec. Pub., 167, The Geological Society London, London.

Srivastava, S.P. & Tapscott, C.R., 1986. Plate kinematics of the North Atlantic, in *The Western North Atlantic Region,* pp. 379–404, eds Vogt, P.R. & Tucholke, B.E., The Geology of North America, Vol. M, Geological Society of America, Boulder, CO.

Steel, R.J., Helland-Hansen, W., Kleinspehn, K., Nottvedt, A. & Rye-Larsen, M., 1985. The Teriary strike-slip basins and orogenic belt of Spitsbergen, in *Strike-Slip Deformation, Basin Formation and Sedimentation,* pp. 339–359, eds Biddle, K.T. & Christie-Blick, N., Special Publications Society of Economic Paleontologists and Mineralogists, 37.

Sundvor, E. & Austegard, A., 1990. The Evolution of the Svalbard Margins: synthesis and new results, in *Geological History of the Polar Oceans: Arctic Versus Antarctic,* pp. 77–94, eds Bleil, U. & Thiede, J., Kluwer, Amsterdam.

Sundvor, E., Myhre, A.M., Austegard, A., Haugland, K., Eldholm, O., Gidskehaug, A., 1982. *Marine Geophysical Survey on the Yermak Plateau,* Seismol. Obs. Scientif Report, 7, University of Bergen, Bergen.

Surlyk, F., 1991. Tectonostratigraphy of North Greenland, *Bull. Grønlands geol. Unders.,* **160**, 25–47.

Thompson, R.N. & Gibson, S.A., 1991. Subcontinental mantle plumes, hotspots and pre-existing thinspots, *J. geol. Soc. Lond.,* **147**, 973–977.

Vågnes, E. & Amundsen, H.E.F., 1993. Late Cenozoic uplift and volcanism on Spitsbergen: caused by mantle convection?, *Geology,* **21**, 251–254.

Wernicke, B., 1985. Uniform-sense normal simple shear of the continental lithosphere, *Can. J. Earth Sci.,* **22**, 108–125.

White, R.S. & McKenzie, D.P., 1989. Magmatism at Rift Zones: the generation of volcanic continental margins and flood basalts, *J. geophys. Res.,* **94**, 7685–7729.

Zelt, C.A. & Smith, R.B., 1992. Seismic traveltime inversion for 2-D crustal velocity structure, *Geophys. J. Int.,* **108**, 16–34.